ISSN 0869-5911, Petrology, 2006, Vol. 14, No. 3, pp. 262–283. © Pleiades Publishing, Inc., 2006.
Original Russian Text © O.M. Turkina, A.D. Nozhkin, T.B. Bayanova, 2006, published in Petrologiya, 2006, Vol. 14, No. 3, pp. 282–303.

Sources and Formation Conditions of Early Proterozoic Granitoids from the Southwestern Margin of the Siberian Craton

O. M. Turkina[a], A. D. Nozhkin[a], and T. B. Bayanova[b]

[a] *Institute of Geology, pr. Akademika Koptyuga 3, Novosibirsk, 630090 Russia*
e-mail: turkina@uiggm.nsc.ru
[b] *Geological Institute, Kola Research Center, Russian Academy of Sciences, ul. Fersmana 14, Apatity, Murmanskaya oblast, 184209 Russia*
e-mail: bayanova@geoksc.apatity.ru

Received January 20, 2005

Abstract—Three stages of Early Proterozoic granitoid magmatism were distinguished in the southwestern margin of the Siberian craton: (1) syncollisional, including the formation of migmatites and granites in the border zone of the Tarak massif; (2) postorogenic, postcollisional, comprising numerous granitoid plutons of diverse composition; and (3) intraplate, corresponding to the development of potassic granitoids in the Podporog massif. Rocks of three petrological and geochemical types (S, I, and A) were found in the granitoid massifs. The S-type granites are characterized by the presence of aluminous minerals (garnet and cordierite), and their trace element distribution patterns and Nd isotopic parameters are similar to those of the country paragneisses and migmatites. Their formation was related to melting under varying H_2O activity of aluminous and garnet–biotite gneisses at $P \geq 5$ kbar and $T < 850$°C with a variable degree of melt separation from the residual phases. The I-type tonalites and dioritoids show low relative iron content, high concentrations of CaO and Sr, fractionated REE distribution patterns with $(La/Yb)_n = 11–42$, and variable depletion of heavy REE. Their parental melts were derived at $T \geq 850$°C and $P > 10$ and $P < 10$ kbar, respectively. According to isotopic data, their formation was related to melting of a Late Archean crustal (tonalite–diorite–gneiss) source with a contribution of juvenile material ranging from 25–55% (tonalites of the Podporog massif) to 50–70% (dioritoids of the Uda pluton). The most common A-type granitoids show high relative iron content; high concentration of high-field-strength elements, Th, and light and heavy REE; and a distinct negative Eu anomaly. Their primary melts were derived at low H_2O activity and $T \geq 950$°C. The Nd isotopic composition of the granitoids suggests contributions to the magma formation processes from ancient (Early and Late Archean) crustal (tonalite–diorite–gneiss) sources and a juvenile mantle material. The contribution of the latter increases from 0–35% in the granites of the Podporog and Tarak massifs to 40–50% for the rocks of the Uda and Shumikha plutons. The main factors responsible for the diversity of petrological and geochemical types of granitoids in collisional environments are the existence of various fertile sources in the section of the thickened crust of the collisional orogen, variations in magma generation conditions (α_{H_2O}, T, and P) during sequential stages of granite formation, and the varying fraction of juvenile mantle material in the source region of granitoid melts.

DOI: 10.1134/S0869591106030040

INTRODUCTION

Early Proterozoic (1.95–1.75 Ga) granitoids are common in all Early Precambrian cratons, where they are confined to systems of collisional and accretionary orogens formed by the amalgamation of Archean crustal terranes into the structure of the Early Proterozoic supercontinent and accretion of juvenile crust along its margin. Accretionary orogens with fragments of island arcs, ophiolites, and sedimentary basins contain a characteristic association of tonalites, granodiorites, and granites, whose compositions correspond to I-type granitoids. These granitoids usually have positive ε_{Nd} and low $^{87}Sr/^{86}Sr$ values suggesting that the main source of felsic melts was the Early Proterozoic juvenile crust with a variable but generally minor contribution of Archean crustal material (Patchett and Arndt, 1986; Nurmi and Haapala, 1986; Whalen, 1998).

Granitoid batholiths are typical structural units of extensively eroded Early Proterozoic collisional orogens. One of the largest belts of Early Proterozoic granitoids (Fig. 1) marks the Southern Yenisei and Prisayanskii inliers of the Siberian craton along its modern southwestern margin. Environments related to the collision of island-arc and continental terranes accompanied by intracrustal melting owing to radiogenic heating or ascent of mantle material are very productive in terms of granite magmatism (Sylvester, 1998; Rozen and Fedorovskii, 2001). Such settings are peculiar in that tremendous volumes of granitoids of various petrochemical types are developed there in response to collision within a relatively narrow time range. Within the

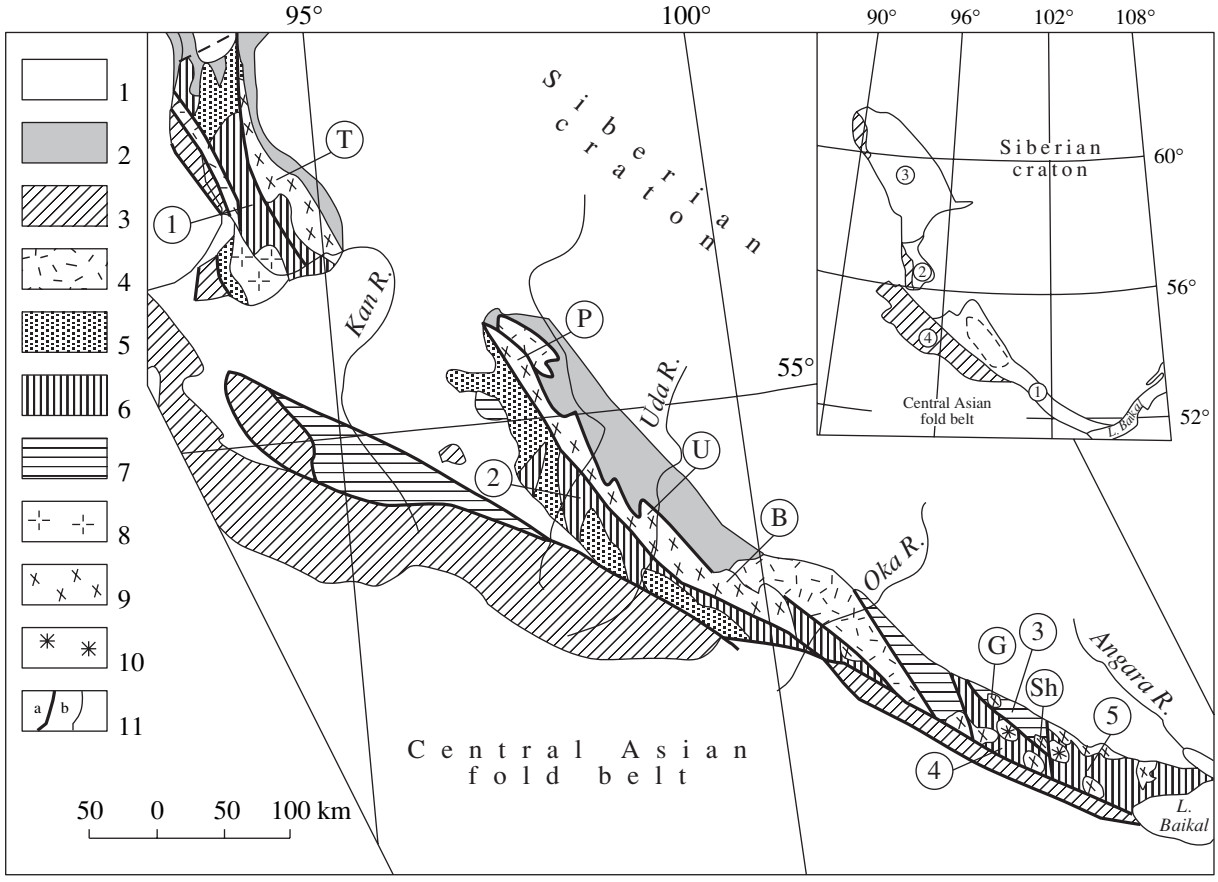

Fig. 1. Sketch map showing the distribution of Early Proterozoic granitoids in the southwestern margin of the Siberian craton. (1) Phanerozoic deposits of the Central Asian fold belt and the cover of the Siberian craton; (2) Late Riphean and Vendian sedimentary deposits; (3) complexes of the Neoproterozoic accretionary belt; (4) Early Proterozoic metasedimentary–volcanic deposits; (5) Early Proterozoic metasedimentary deposits; (6) Early Precambrian granulite gneiss complexes; (7) Early Precambrian granite–greenstone complexes; (8)–(10) granitoid complexes: (8) Early Paleozoic, (9) Early Proterozoic, and (10) Late Archean; (11a) fault zones; and (11b) other geologic boundaries. Tectonic blocks (numerals in circles): 1, Angara–Kan; 2, Biryusa; 3, Onot; 4, Kitoi; and 5, Irkutnyi. Granite massifs (letters in circles): T, Tarak; P, Podporog; U, Uda; B, Barbitai; G, Girgintuiskii; and Sh, Shumikha. The inset shows Early Precambrian inliers of the craton basement: 1, Prisayanskii; 2, Southern Yenisei; 3, Proterozoic fold–and-thrust region of the Yenisei Range; and 4, Neoproterozoic accretionary belt. The shaded area is the location of the map in Fig. 2.

accepted geochemical classifications (Chappell and White, 1974; Whalen et al., 1987; etc.), collisional granitoids range in composition from peraluminous S-type granites, which are typical of this setting and related to the stage of crustal thickening, to I- and A-types granites, which are mainly formed under extensional conditions caused by the instability of the thick crust of the collisional orogen and thinning of the lithosphere as a result of delamination (Sylvester, 1998). The goal of this study was the analysis of possible reasons for the diversity of collisional granitoids, including the difference in the composition of their crustal sources and *P–T* conditions of magma formation and a variable contribution of mantle material at the level of melt generation. The main problems addressed in this study are (1) the analysis of the composition and petrochemical systematics of granitoids, (2) determination of possible melt sources and conditions of magma formation, and (3) estimation of the role of various factors in the genesis of granitoids.

GEOLOGIC SETTING AND AGE OF GRANITOIDS

Large massifs of Early Proterozoic granitoids from the marginal basement inliers (Prisayanskii and Southern Yenisei) of the southwestern margin of the Siberian craton (Fig. 1) have mainly intrusive contacts with the Early Precambrian country complexes and are interpreted as postorogenic or postkinematic on the basis of their structural position (Levitskii et al., 2002; Donskaya et al., 2002; Nozhkin et al., 2003). New results obtained recently by various authors on the age of the Early Proterozoic granitoids are summarized in Table 1.

In the Angara–Kan and Biryusa blocks, the granitoids are hosted by granulite-gneiss and gneiss complexes. The granulite-gneiss complex (Kan Group) of

Table 1. Geologic setting, composition, and age of the Early Proterozoic granitoids of the southwestern margin of the Siberian craton

Stage	Massif	Block	Rocks	Age, Ma	Reference
Syncollisional	Tarak	Angara–Kan	Garnet- and cordierite-bearing granites and gneissic granites	1900 ± 10	Bibikova et al., 1993
Collisional posttectonic	Tarak	Angara–Kan	Granites and leucogranites	1837 ± 3	Nozhkin et al., 2003
	Podporog	Biryusa	Tonalites	1869 ± 10	Turkina et al., 2003
	Uda	Biryusa	Quartz diorites and monzodiorites	1859 ± 10	This work
	Barbitai	Biryusa	Granodiorites, syenogranites, and granites	1858 ± 20	Levitskii et al., 2002
	Shumikha	Onot	Quartz diorites and monzodiorites, granites, and leucogranites	1861 ± 1	Donskaya et al., 2002
	Girgintuiskii	Onot	Granodiorites, syenogranites, and granites	1869 ± 6	Kirnozova et al., 2003
Anorogenic	Podporog	Biryusa	Granites and leucogranites	1747 ± 4	Turkina et al., 2003
	Small massifs	Angara–Kan	Hypersthene granites	1734 ± 4	Bibikova et al., 2001a

the Angara–Kan block (Fig. 1) is composed of basic schists (metabasalts), plagiogneisses, and two-feldspar hypersthene-bearing gneisses (metadacites and metarhyodacites), which are changed upsection by metasedimentary garnet–biotite and aluminous gneisses (Nozhkin and Turkina, 1993). The rocks are metamorphosed under granulite-facies conditions (P from 9–10 to 7–8 kbar and T from 950–1000 to 800°C) (Nozhkin and Turkina, 1993). The metamorphism was accompanied by the formation of migmatites and syncollisional granitoids or autochthonous charnockites at various levels of the crustal section. The time of metamorphic events was estimated as 1900 ± 10 Ma (Bibikova et al., 1993). The development of the postcollisional potassium granites of the Tarak pluton occurred at 1837 ± 3 Ma (Nozhkin et al., 2003). The age of the latest cutting bodies and veins of allochthonous charnockite (kuzeevites) is 1734 ± 4 Ma (Bibikova et al., 2001a).

The structure of the Biryusa block (Fig. 2) is controlled by extended linear uplifts bounded mainly by NW–SE trending faults and consisting of gneisses, migmatites, and granite gneisses of the Khailaminskaya Group and grabens filled with Early Proterozoic metasediments of the Neroi Group. The block is bounded to the northeast by a series of thrusts separating the Late Riphean sedimentary deposits of the Prisayanskii trough. The granitoids are confined to basement highs. The metamorphic section of the Khailaminskaya Group is dominated by metasedimentary biotite and garnet–biotite gneisses with occasional biotite and amphibole orthogneisses, aluminous paragneisses, and rare amphibolite layers (metabasic rocks). The rocks are metamorphosed under amphibolite facies conditions and locally contain relics of granulite mineral assemblages. In places, the gneisses are migmatized and granitized with the formation of augen gneisses and granite gneisses with variable compositions from plagiogranitoid to microcline granite. The age of metamorphism was estimated on the basis of $^{207}Pb/^{206}Pb$ ratio of zircon from the biotite gneisses as 1900 ± 30 Ma. The posttectonic tonalites of the Podporog massif and the granitoids of the Barbitai massif have an age of ~1870 Ma (Levitskii et al., 2002; Turkina et al., 2003). The dioritoids of the Uda massif were formed nearly contemporaneously, which is suggested by their U–Pb zircon age of 1859 ± 10 Ma (Table 2, Fig. 3). Three zircon populations were separated for the U–Pb dating of the quartz diorites. The zircons are semitransparent prismatic crystals of a hyacinth or zircon habit with an aspect ratio of ~5 or their fragments. The three-point discordia (Fig. 3) yields an upper intercept age of 1859 ± 10 Ma. One of the three fractions shows almost concordant values of isotopic ratios corresponding to an age of 1858 ± 4 Ma, which is identical within the measurement error to the upper intercept age. These results allow us to accept a value

Fig. 2. Geological sketch map of the northwestern part of the Biryusa block, after the author's materials and the data of geological mapping by Irkutsk Geological Survey (Anisimova et al., 1982). Sedimentary, volcanosedimentary, and metamorphic complexes: (1) Devonian sediments; (2) Late Riphean and Vendian sediments (Karagasskaya and Oselochnaya groups); (3) Early Proterozoic metasedimentary–volcanic sequences (Sublukskaya Group); (4) Early Proterozoic metacarbonate–terrigenous rocks (Neroi Group); (5) Archean gneisses (Khailaminskaya Group); (6) Early Precambrian migmatite–granite gneiss complex (Khadaminskii). Intrusive complexes: (7) Early Paleozoic granite–syenogranite; (8)–(12) Early Proterozoic granitoids: Uriksko–Iiskii and Elash grabens (8, granites and leucogranites; 9, granodiorites and plagiogranites), Early Precambrian basement structures (10, granites; 11, tonalites; 12, granitoids of various compositions); (13) Early Precambrian charnockite; (14) Early Precambrian metagabbroid; (15)–(17) geologic boundaries: (15) fault; (16) unconformity, and (17) other boundaries. Granite massifs (letters in circles): P, Podporog and U, Uda.

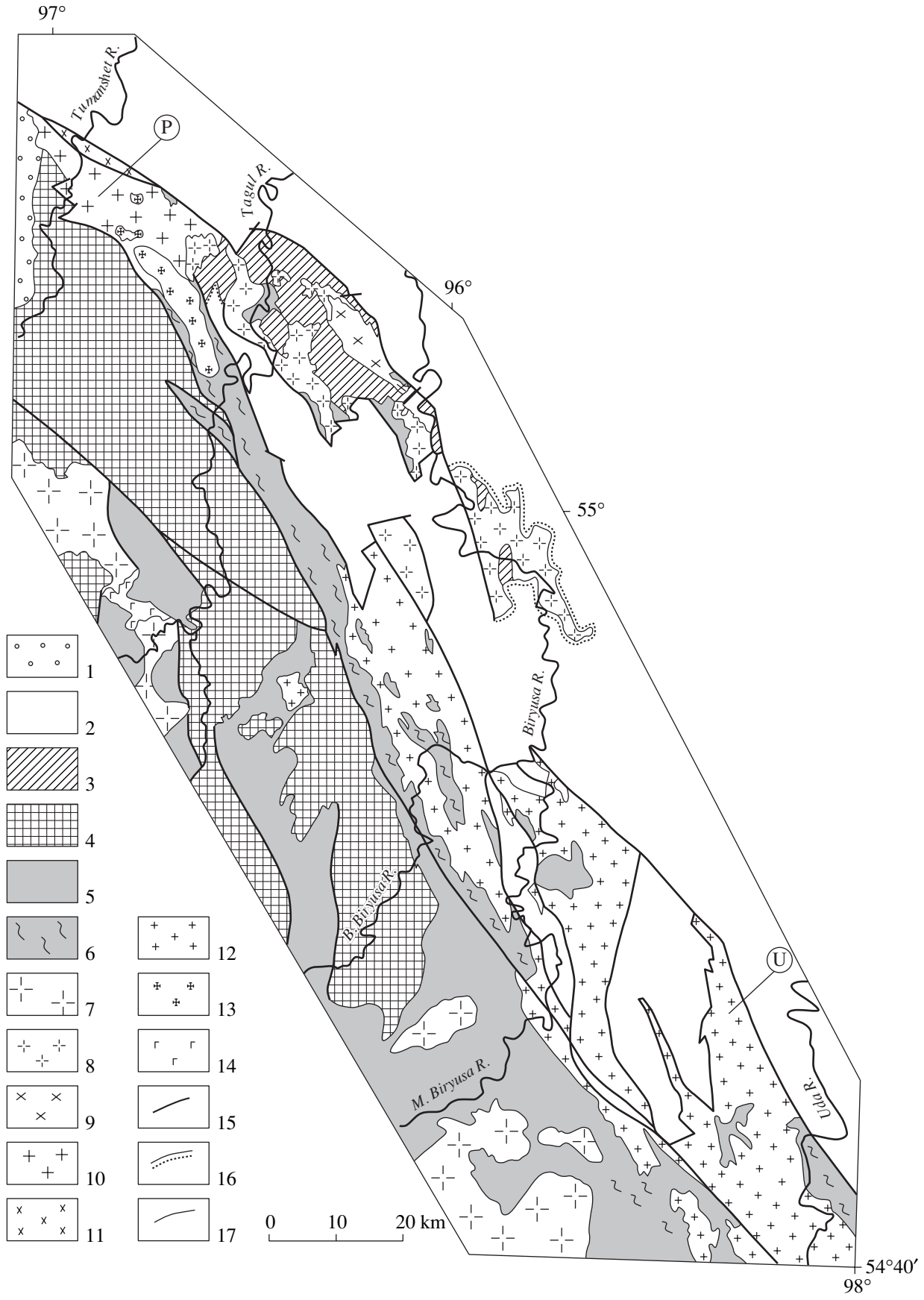
97°
96°
55°
54°40′
98°
Tumanshet R.
Tagul R.
Biryusa R.
B. Biryusa R.
M. Biryusa R.
Uda R.
P
U
1
2
3
4
5
6
7
8
9
10
11
12
13
14
15
16
17
0
10
20 km

Table 2. Results of U–Pb isotopic investigations of zircon from the quartz diorite of the Uda massif

No.	Size fraction, μm	Weight, mg	Content, ppm		Isotope ratio		
			Pb	U	$^{206}Pb/^{204}Pb$	$^{207}Pb/^{206}Pb$	$^{208}Pb/^{206}Pb$
1	>100	0.55	147.8	413.9	1383	0.1234 ± 2	0.1077 ± 6
2	–100+75	0.80	208.3	632.2	1183	0.1229 ± 1	0.1371 ± 2
3	<75	0.75	145.0	450.8	2286	0.1172 ± 2	0.1401 ± 2

No.	Size fraction, μm	Isotope ratio		Rho	Age, Ma		
		$^{207}Pb/^{235}U$	$^{206}Pb/^{238}U$		$^{207}Pb/^{235}U$	$^{206}Pb/^{238}U$	$^{207}Pb/^{206}Pb$
1	>100	5.2210 ± 2	0.3333 ± 9	0.84	1856 ± 5	1854 ± 5	1858 ± 4
2	–100+75	4.6056 ± 1	0.2998 ± 6	0.76	1750 ± 5	1690 ± 3	1823 ± 3
3	<75	4.5279 ± 1	0.2952 ± 1	0.86	1736 ± 3	1668 ± 3	1820 ± 2

of 1859 ± 10 Ma as an age estimate for the magmatic crystallization of zircon in the diorites. The later potassium granites of the Podporog intrusion were dated at 1747 ± 4 Ma (Turkina et al., 2003). The formation of the crust of the Angara–Kan and Biryusa blocks was confined to the Late Archean stage on the basis of the model age of gneisses hosting the granitoids, T(DM-2st) = 2.7–2.9 Ga.

The structure of the Onot block of the Prisayanskii inlier is composed of tectonic blocks and sheets composed of Early Archean (3287 ± 8 Ma; Bibikova et al., 2001b) plagiogneisses and gneissic plagiogranites of the tonalite–trondhjemite composition. They are regarded as a basement complex for the stratified sequence of the Onot greenstone belt (Nozhkin et al., 2001). The metasedimentary–volcanic sequences of the greenstone belt include biotite and amphibole–biotite orthogneisses overlain by intercalating amphibolites, amphibole schists, aluminous gneisses, dolomite marbles, and iron formations. According to the results of Ar–Ar dating of amphibole from the orthogneisses of the lower part of the section, the metamorphism occurred 1879.6 ± 17.1 Ma ago (our unpublished data). In the Onot block, the Early Proterozoic stage produced the granitoids of the Shumikha and Girgintuiskii massifs with an age of ~1860 Ma (Donskaya et al., 2002; Levitskii et al., 2002).

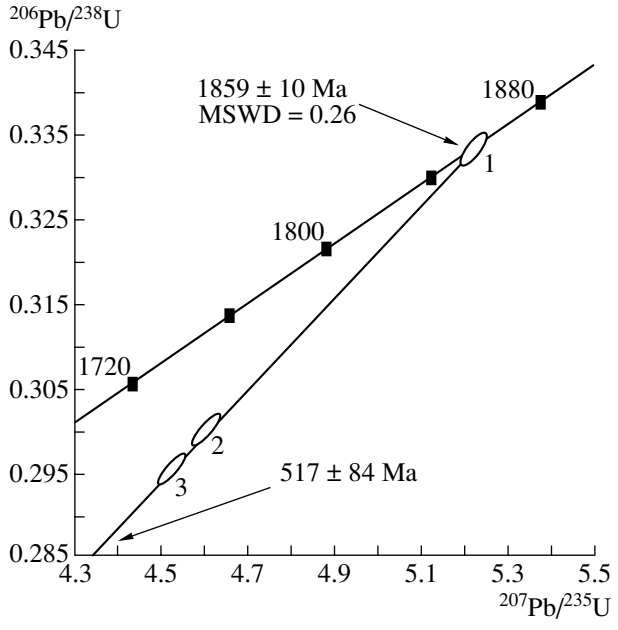

Fig. 3. Concordia diagram for zircons from the quartz diorite (sample 17-01) of the Uda massif. The labels of points correspond to analysis numbers in Table 2.

Based on the results of U–Pb dating, three stages of granite magmatism corresponding to collisional and intraplate settings were distinguished (Table 1). The first stage included the formation of migmatites and syncollisional autochthonous granitoids of the contact and boundary zones of the Tarak massif, the age of which is similar to that of metamorphism (1900 ± 10 Ma). During the second postorogenic, postcollisional stage, a wide spectrum of granitoids from tonalite and diorite to microcline granite was generated within a narrow age interval of ~1870–1840 Ma. The granitoids of the third anorogenic stage have an age of 1747–1734 Ma and are represented by potassic-series rocks.

STRUCTURE AND COMPOSITION OF GRANITOID MASSIFS

The Tarak massif in the eastern part of the Angara–Kan block extends northwest from the Kan River over 150 km at a width of 10–20 km (Fig. 1). It is overlain by Late Precambrian and Devonian sedimentary deposits in the east and south, respectively. The western contact with the country paragneisses and migmatites is intrusive and occasionally tectonic. The massif has a complex structure formed by two types of granitoids, which have different tectonic setting and origin but are spatially superimposed within a single massif. The central and eastern parts of the Tarak pluton are composed

of massive porphyritic and granoblastic biotite granites and leucogranites of the main phase with an age of 1837 ± 3 Ma. Their characteristic accessory minerals are monazite, zircon, apatite, native iron (Arbuzov and Novoselov, 1995), and moissanite (Datsenko, 1984), the presence of which indicates that the rocks were formed under reduced conditions. The western border zone of the massif, 3–4 km wide, is composed of heterogeneous garnet- and cordierite-bearing gneissic biotite granites, granodiorites, and plagiogranites, which often have gneissic structures and sometimes grade into the rocks of the outer contact zone. Such relationships are indicative of the autochthonous character of these granitoids. The contact zone, up to 5 km wide, contains abundant venite and arterite migmatites formed after garnet–biotite and aluminous cordierite- and sillimanite-bearing gneisses. There are also widespread vein bodies nearly conformable with the gneissic and migmatitic banding of the country complexes. The veins are composed of gneissic granitoids, which are mineralogically and chemically identical to the rocks from the border zone of the massif. The heterogeneous, often gneissic granitoids of the border zone and their vein analogs from the contact aureole are obviously earlier syncollisional rocks similar in age to regional metamorphism (~1900 Ma), whereas the postcollisional granites and leucogranites of the main volume of the Tarak pluton were formed ~60 Ma later. The granites and leucogranites show no evidence for deformation, and the leucogranites have discordant intrusive contacts with the gneissic granites.

The Podporog massif is situated at the northwestern margin of the Biryusa block (Figs. 1, 2). It is bounded to the northeast and southwest by fault zones separating the granitoids from the Early Proterozoic deposits of the Gutara–Tumanshet depression and the Late Riphean deposits of the Prisayanskii trough, respectively. The present-day internal structure of the massif is formed by a series of tectonic slices. The most abundant rocks are coarse-grained porphyritic microcline granites and gneissic granites. The granites usually contain no more than 10% of iron-rich biotite (f = 77–78%) (Bryntsev, 1994). Accessory minerals are ilmenite, titanite, apatite, zircon, allanite, and fluorite. Medium- to coarse-grained tonalites compose a tectonic slice with an apparent thickness of ~4–5 km exposed along the northeastern boundary of the massif and thin tectonic lenses among microcline granites (Turkina, 2005). The tonalites contain 10–15% iron-poor biotite (f = 50–67%) (Bryntsev, 1994) and no more than 5–10% fine-grained microcline; larger porphyroblasts of potassium feldspar occur at the zone of tectonic contact with the granites. Accessory minerals are apatite, zircon, magnetite, and monazite.

The Uda massif is situated in the central part of the Biryusa block (Uda R.) (Fig. 2). In the north and east, it is separated by a regional fault zone from the Late Proterozoic deposits of the Prisayanskii trough. The western boundary of the massif is mostly tectonic; intrusive contacts were observed in places with the Early Precambrian metamorphic rocks of the Khailaminskaya Group, which is dominated there by biotite and amphibole–biotite gneisses with amphibolite layers. Near the tectonic contacts, the granitoids of the Uda pluton show a distinct gneissic structure, are affected by the development of microcline porphyroblasts, and are transformed into augen gneisses and gneissic granites. The occurrence of numerous roof pendants of metamorphic rocks among the granitoids suggests a shallow erosion level of the massif. Two types of rocks were distinguished on the basis of mineral composition: more abundant biotite (*amphibole*) granites and leucogranites with accessory apatite, zircon, and allanite and minor amphibole (*biotite*) quartz diorites and monzodiorites with typical accessory titanite. Syenogranites were found in the vein bodies.

The Shumikha massif is located in the junction zone between the Onot and Kitoi blocks of the Prisayanskii inlier (Fig. 1) and shows intrusive contacts against the metasedimentary and volcanic complexes of the Onot greenstone belt. The pluton exhibits considerable variations in granitoid composition: from amphibole and biotite–amphibole quartz diorite and granodiorite composing the first phase to mainly biotite granites and leucogranites of the second phase (Levitskii et al., 2002; Donskaya et al., 2002). Potassium feldspar (microcline) occurs in all the rock varieties from diorite to leucogranite. Main accessory minerals are apatite, zircon, titanite, and allanite.

GEOCHEMISTRY OF GRANITOIDS

Analytical Methods

The rocks were analyzed at the Analytical Center of the Joint Institute of Geology, Geophysics, and Mineralogy, Siberian Division, Russian Academy of Sciences, Novosibirsk. Major elements were determined by X-ray fluorescence; rare earth elements, by instrumental neutron activation analysis and ICP-MS; and other trace elements, by SR XRD. The Sm–Nd and U–Pb isotopic analyses were obtained at the laboratory of geochronology of the Geological Institute, Kola Research Center, Russian Academy of Sciences, Apatity using the methods described by Bayanova (2004). Isotopic investigations were performed on a Finnigan MAT-262 (RPQ) seven-channel mass spectrometer running in static mode. The laboratory blanks were 0.06 ng Sm, 0.3 ng Nd, 0.08 ng Pb, and 0.04 ng U. The isotopic investigation of zircons was performed by the method of Krogh (1973) for microscopic zircon samples. The concentrations of U and Pb were determined by the isotope dilution method using a mixed ^{208}Pb + ^{235}U isotopic tracer. Isotopic ages were calculated using the programs of Ludwig (1991, 1999). The data were corrected for common lead using the model of Stacey and Kramers (1975). The errors of U–Pb ratios were accepted using the IGFM-87 standard and calculated

Table 3. Concentrations of major (wt %) and trace elements (ppm) in representative samples of Early Proterozoic granitoids from the southwestern margin of the Siberian craton

Component	First group						Second group				
	Tarak massif						Podporog massif				
	1	2	3	4	5	6	7	8	9	10	11
	20-73*	209-72	1-73	213-72	19-73	48-73	24-00	22-00	20-00	21-00	521-81
SiO_2	64	67.39	68.50	70.36	71.66	71.86	63.39	64.55	62.28	64.52	65.24
TiO_2	0.5	0.50	0.57	0.38	0.56	0.55	0.654	0.847	0.794	0.717	0.653
Al_2O_3	15.8	15.21	14.50	14.51	13.86	12.04	16.65	15.73	17.36	16.58	16.15
$Fe_2O_3^*$	7.00	5.89	5.80	4.86	4.00	4.54	5.83	6.39	5.55	5.26	5.05
MnO	0.1	0.04	0.05	0.03	0.06	0.06	0.073	0.066	0.066	0.058	0.075
MgO	2.85	1.24	1.70	0.96	1.03	2.13	2.09	1.76	1.84	1.74	1.75
CaO	3	2.36	1.60	1.53	3.26	3.66	4.26	4.09	4.14	4.49	3.26
Na_2O	2.05	2.54	2.25	2.70	2.18	2.08	3.63	3.24	3.23	3.23	2.97
K_2O	3.55	4.23	4.35	4.01	2.55	2.25	1.63	2.22	2.53	1.85	2.44
P_2O_5	0.15	0.17	0.10	0.20	0.17	0.17	0.241	0.176	0.264	0.175	0.264
LOI	1.72	1.07	0.98	0.71	0.75	0.75	1.21	0.42	1.15	0.38	1.72
Total	100.7	100.2	99.94	100.3	100.1	99.73	99.73	99.52	99.26	99.08	99.57
Th	26.2	22.5	23.4	26.5	14.5	14.5	18.4	2.6	9.1	0.8	1.4
U	1.2	1.5	3.2	1.8	1.5	1.5	1.9	1	0.7	0.5	0.6
Rb	170	190	196	210	80	115	97	185	162	126	121
Ba	406	557	710	418	143	607	640	310	560	660	327
Sr	120	107	200	118	152	170	509	322	373	420	347
La	32	43	47	46	46	37	80	20.5	60	8.8	16
Ce	51	67	100	82	70	66	132	40	105	18	30
Nd	19	39	44	27	25	–	58	17	46.5	9.8	18
Sm	2.8	8.9	8.6	3.4	4.1	5.4	8.2	3.2	7.2	1.9	4.8
Eu	1.2	0.7	1.1	1.7	1.2	1.2	1.65	1	1.3	1.3	1.5
Gd	–	7.6	6.3	–	–	5	4.2	3	4.5	2	4.5
Tb	–	0.7	1	–	–	1	0.63	0.42	0.6	0.36	0.68
Tm	–	–	0.45	–	–	0.45	–	–	–	–	–
Yb	–	3.2	2.7	–	–	2.7	1.5	0.73	0.3	0.95	0.27
Lu	–	0.3	0.4	–	–	0.35	0.2	0.08	0.04	0.1	0.022
Zr	60	180	120	185	255	140	225	170	212	170	155
Hf	–	5.6	5.1	–	–	4.8	5.4	5.2	5.2	4.7	4
Ta	–	1.6	1.4	–	–	2	0.6	1.2	1.1	0.65	0.8
Nb	12	–	–	13.4	14	–	11	8.8	15.5	9	10
Y	25.5	22	23	23	18	16	18.9	16	16.4	13.5	13
$(La/Yb)_n$	–	9.1	11.7	–	–	9.2	36.0	18.9	134.8	6.2	40.0
Eu/Eu*	–	0.25	0.44	–	–	0.69	0.77	0.97	0.65	2.03	0.97
Sr/Y	4.7	4.9	8.7	5.1	8.4	10.6	26.9	20.1	22.7	31.1	26.7

Table 3. (Contd.)

Component	Second group				Third group						
	Uda massif				Tarak massif					Uda massif	
	12	13	14	15	16	17	18	19	20	21	22
	17-01	16-01	24-01	9-01	312-79	313-79	1-98	314-79	306-79	32-01	33-01
SiO_2	56.08	57.67	61.74	65.1	69.38	70.80	70.92	71.58	73.15	70.5	73.94
TiO_2	0.663	0.66	0.704	0.278	0.57	0.50	0.32	0.60	0.25	0.321	0.217
Al_2O_3	15.81	15.82	16.24	16.65	14.26	14.38	14.52	13.30	13.70	13.78	13.26
$Fe_2O_3^*$	6.67	6.53	5.91	3.18	4.06	3.78	2.77	3.77	1.86	3.26	2.13
MnO	0.14	0.143	0.11	0.059	0.04	0.02	0.03	0.09	0.02	0.075	0.057
MgO	6.6	6	2.56	0.79	0.60	0.39	0.72	0.50	0.28	0.55	<0.1
CaO	7.78	7.24	4.95	1.31	1.42	1.00	1.06	1.50	0.65	1.09	0.38
Na_2O	1.83	1.83	2.88	4.49	2.30	2.25	2.63	2.27	2.60	2.28	3.1
K_2O	2.14	1.87	3.6	6.46	6.00	6.00	5.94	5.54	5.55	6.64	5.56
P_2O_5	0.196	0.174	0.174	0.069	0.24	0.26	0.10	0.16	0.12	0.075	0.035
LOI	1.6	1.65	1.6	0.86	0.92	0.81	0.64	0.96	1.50	0.87	0.96
Total	99.51	99.59	100.57	99.25	99.5	99.92	99.65	99.95	99.68	99.44	99.64
Th	4.5	8	16	17	71.0	77.0	46.0	89.0	86.0	19	18
U	0.3	1.7	1.8	2	3.5	3.0	4.2	1.6	8.2	2.4	1.7
Rb	103	68	111	183	190	266	342	260	350	210	186
Ba	454	285	820	772	460	313	426	375	430	1393	947
Sr	416	363	393	248	40	63	78	75	50	222	173
La	27	38	41	60	85	100	61	95	90	52	49
Ce	51	63	87	83	155	202	130	200	180	112	69
Nd	26	27	35	28	–	84	56	105	84	38	28
Sm	4	4.7	6.3	3.6	13.7	18.1	10.5	24	17	6.5	4.5
Eu	1.24	1	1.4	1.8	0.7	0.64	0.81	0.62	0.6	0.98	1.13
Gd	3	4.1	5.6	2.5	12	12.2	6.4	17.2	10.4	5.7	3.4
Tb	0.38	0.53	0.73	0.4	1.8	1.7	0.88	2.3	1.75	0.73	0.37
Tm					0.6	0.43	0.17	0.6	0.9	0.41	0.23
Yb	1.2	1.7	2.5	1.4	3.3	2.7	0.78	3.2	6	2.8	1.5
Lu	0.21	0.25	0.38	0.17	0.44	0.33	0.1	0.43	0.87	0.43	0.2
Zr	171	109	201	176	400	500	390	730	480	279	146
Hf	3.5	3.1	6.1	4	11.5	10	6.4	15	14	8.3	6
Ta	0.55	0.83	0.83	0.76	1.1	1.1	1.1	1.5	2.3	1.1	1.2
Nb	7.5	8.5	11	10.9	–	–	16	–	–	8.7	11
Y	16.4	16	21	16.3	58	34	19	80	54	22	15.9
$(La/Yb)_n$	15.2	15.1	11.1	28.9	17.4	25.0	52.7	20.0	10.1	12.5	22.0
Eu/Eu*	1.05	0.68	0.71	1.74	0.16	0.12	0.28	0.09	0.13	0.48	0.85
Sr/Y	25.4	22.7	18.7	15.2	0.7	1.9	4.1	0.9	0.9	10.1	10.9

Table 3. (Contd.)

Component	Third group											
	Uda massif		Podporog massif					Shumikha massif				
	23	24	25	26	27	28	29	30	31	32	33	34
	25-01	6-01	18-00	14-00	17-00	510-81	508-81	3-03	6-03	4-03	13-95	16-95
SiO_2	74.93	76.66	67.31	69.43	70.3	71.5	73.71	63.96	65.19	66.72	69.35	70.94
TiO_2	0.113	0.156	0.83	0.618	0.565	0.675	0.422	1.247	1.058	1.039	0.762	0.477
Al_2O_3	13.31	11.67	13.55	13.71	12.86	12.22	12.14	13.72	13.67	13.03	13.67	13.75
$Fe_2O_3^*$	1.5	1.75	6.18	5.05	5.24	4.36	2.57	7.72	6.66	6.64	4.82	4.2
MnO	0.041	0.044	0.07	0.06	0.05	0.05	0.03	0.10	0.09	0.09	0.08	0.06
MgO	0.21	0.37	0.84	0.73	0.81	0.68	0.38	1.46	1.2	1.21	0.86	0.56
CaO	0.39	0.14	2.65	1.86	1.56	1.78	0.79	3.29	2.84	3	2.39	1.29
Na_2O	2.43	1.02	2.62	2.37	2.38	2.26	2.32	3.59	3.17	3.42	2.97	2.96
K_2O	5.84	7.42	5.32	5.9	5.7	5.17	6.77	4.14	4.25	4.13	4.13	4.97
P_2O_5	0.031	0.035	0.201	0.135	0.123	0.152	0.064	0.411	0.354	0.344	0.287	0.151
LOI	0.82	0.68	0.3	0.12	0.2	0.86	0.76	0.59	0.88	0.67	0.91	0.69
Total	99.62	99.95	99.97	100.1	99.85	99.71	99.96	100.3	99.48	100.4	100.3	100.1
Th	13	48	23.9	45	38.5	42	59	18.8	16.4	19.5	25	40.3
U	0.8	1.6	1.1	1.8	1.6	3.2	4.2	2.8	3	2.9	5.6	7.2
Rb	190	190	220	306	369	270	262	168	155	144	204	258
Ba	608	386	910	581	550	560	370	990	1345	1010	930	420
Sr	168	84	73	73	75	60	40	190	190	170	140	90
La	22	80	90	85	92	104	55	114	127	76	106	93
Ce	36	170	180	168	180	187	105	205	190	160	192	164
Nd	14	95	76	73	73	78	48	90	90	68	73	62
Sm	1.6	14.5	12.8	12	12	17	9.4	17	15.6	13.5	12.5	11.6
Eu	0.65	3.7	1.4	0.93	1	0.95	0.66	2.1	2.3	1.95	1.73	1.2
Gd	1	9.8	14	12	13	15	9	14	15	13	12.5	12
Tb	0.18	1.3	2	1.7	1.9	2.1	1.51	2.2	1.75	1.65	1.7	1.7
Tm	0.068	0.32	0.6	0.93	0.6	0.84	0.88	1.15	0.72	0.8	1	1
Yb	0.5	2.4	6.5	5.6	5.2	4.7	4.3	8	6.3	6	7.2	7.5
Lu	0.095	0.36	0.93	0.78	0.7	0.58	0.61	1.06	0.85	0.86	0.95	1
Zr	63	93	440	413	338	402	447	370	290	270	200	560
Hf	2.5	3.5	12	11	10	12.3	12.6	13.6	8	8	8	9.8
Ta	0.37	0.37	1.5	1.6	1.1	0.94	0.88	1.9	1.8	1.8	3.3	4.1
Nb	3.5	3.4	20	20	25	21	18	22	17	17	19	24
Y	7.2	6.2	59	59	77	63	42	56	46	43	49	58
La/Yb_n	29.7	22.5	9.3	10.2	11.9	14.9	8.6	9.6	13.6	8.5	9.9	8.4
Eu/Eu*	1.47	0.90	0.32	0.23	0.24	0.18	0.22	0.36	0.40	0.44	0.42	0.31
Sr/Y	23.3	13.5	1.2	1.2	1.0	1.0	1.0	3.4	4.1	4.0	2.9	1.6

Note: $Fe_2O_3^*$ is total iron calculated as Fe_2O_3. $(La/Yb)_n$ is the chondrite-normalized ratio (Boynton, 1984). Dashes denote no data. Rocks: 1 and 2, granodiorites; 3 and 4, low-alkali granites; 5 and 6, plagiogranites; 7 and 9, quartz diorites; 8, 10, and 11, tonalites; 12, diorite; 13, quartz diorite; 14, quartz monzodiorite; 15, alkali quartz syenite; 16–18, subalkaline granites; 19, granite; 20, subalkaline leucogranite; 21, subalkaline granite; 22–24, subalkaline leucogranites; 25, granodiorite; 26 and 27, subalkaline granites; 28, granite; 29, subalkaline leucogranite; 30 and 31, quartz monzodiorites; 32, granodiorite; and 33 and 34, granites.
* Sample number.

Table 4. Geochemical parameters of the Early Proterozoic granitoids

Massif	SiO_2, wt %	A/CNK	FeO*/(FeO* + MgO)	K_2O, wt %	Rb, ppm	Sr, ppm	Zr, ppm	Nb, ppm	Th, ppm	Ce, ppm	Femic minerals
S-type granites											
Tarak	64–72	**1.1–1.5**	0.7–0.8	2.3–4.4	80–200	110–200	60–260	12–14	14–27	50–100	*Bt*, *Grt*, *Crd*
I-type granites											
Podporog	63–65	1.0–1.2	0.64–0.77	**1.6–2.5**	60–180	**300–500**	160–220	9–15	**2–18**	30–130	*Bt*
Uda	56–65	0.8–1.1	0.5–0.8	**1.9–3.8**	100–130	**250–420**	110–200	7–11	**4–17**	50–90	*Bt*, *Hbl*
A-type granites											
Tarak	68–73	1.1–1.2	**0.8–0.9**	**4.5–6.0**	180–350	40–80	**390–730**	**16**	46–90	**130–200**	*Bt*
Podporog	67–74	0.9–1.1	**0.75–0.9**	**5.2–6.8**	220–370	40–70	**340–450**	**18–25**	24–60	**100–190**	*Bt*
Uda	70–75	1.0–1.3	**0.74–0.9**	**6.0–7.5**	150–190	80–220	**60–280**	**9–11**	13–50	**40–170**	*Bt*, *Hbl*
Barbitai*	64–74	1.0–1.1	**0.8–0.9**	**3.7–6.1**	110–250	170–480	**200–410**	**6–27**	–	**100–220**	*Bt*, *Hbl*
Shumikha	64–74	0.8–1.1	**0.83–0.87**	**4.0–5.0**	110–270	80–300	**170–370**	**10–26**	16–40	**160–200**	*Bt*, *Hbl*
Girgintuiskii*	65–74	0.8–1.1	**0.83–0.86**	**4.1–5.0**	110–270	80–300	**170–360**	**10–26**	–	**100–180**	*Bt*, *Hbl*

Note: A/CNK = $Al_2O_3/(CaO + Na_2O + K_2O)$, mol % (Clarke, 1981). Mineral abbreviations: *Bt*, biotite; *Hbl*, hornblende; *Grt*, garnet; and *Crd*, cordierite. Concentrations of elements and their ratios typical of the given granitoid type are shown in bold.
* After Levitskii et al. (2002).

for a level of 0.5%. The accuracy of measurement was ±0.2% (2σ) for Sm and Nd concentrations and $^{147}Sm/^{144}Nd$ ratios. The accuracy of $^{143}Nd/^{144}Nd$ ratios (2σ) is shown in Table 5. During our analytical measurements, the average $^{143}Nd/^{144}Nd$ values for standard samples were 0.511833 ± 6 (2σ) for La Jolla (N = 11) and 0.512072 ± 2 (2σ) for Jindi1 (N = 44). The values of ε_{Nd} and model ages T(DM) were calculated using the modern values for the chondrite uniform reservoir (CHUR), $^{143}Nd/^{144}Nd$ = 0.512638 and $^{147}Sm/^{144}Nd$ = 0.1967, and the depleted mantle (DM), $^{143}Nd/^{144}Nd$ = 0.513151 and $^{147}Sm/^{144}Nd$ = 02136.

Distribution of Major and Trace Elements

Three groups of granitoids were distinguished on the basis of petrographic observations and major- and trace-element systematics (Tables 3, 4).

The first group includes biotite granitoids with garnet and, occasionally, cordierite composing the border zone of the Tarak massif and vein bodies in the contact aureole. In terms of major-element composition, they are peraluminous granodiorites and low-alkali granites with low f = FeO*/(FeO* + MgO) ratios (0.7–0.8) (Fig. 4). Judging from the mineralogical characteristics and distinct peraluminous character of the rocks, they are S-type granites (Chappell and White, 1974). The rare earth element spectra of the granitoids are weakly fractionated, $(La/Yb)_n$ = 9–12, with a pronounced negative Eu anomaly, Eu/Eu* = 0.3–0.7 (Fig. 5a). The concentrations of K_2O and alkali and alkali earth trace elements (Rb, Ba, and Sr), which are mainly incorporated in major rock-forming minerals, correspond to the range of concentrations of these elements in the country gneisses and venite migmatites. The multielement patterns of the gneisses, migmatites, and granites show similar levels of trace element concentrations and similar anomalies: a weak negative Ta anomaly and more pronounced negative anomalies for Ba, Sr, P, and Ti (Fig. 5b). Heavy REE and Y show the highest variations in the gneisses, migmatites, and granitoids, which is related to the variable content of garnet, the main host of these elements.

The second group comprises rocks with predominantly moderately potassic compositions and considerable variations in SiO_2 content, from diorite and tonalite to granodiorite. This group includes tonalites composing a tectonic slice along the northeastern boundary of the Podporog massif (~1870 Ma) and monzodiorites and quartz diorites from the Uda massif (~1860 Ma). The rocks of this group show a calcic or alkali-calcic character, have low f values (0.5–0.8), and elevated CaO and Sr contents (Fig. 4). These compositional features correspond to I-type granites (Chappell and White, 1974). The tonalites of the Podporog massif have the highest Sr/Y ratios (10–36), strongly fractionated REE patterns with $(La/Yb)_n$ = 19–42, and a slight negative Eu anomaly with Eu/Eu* = 0.7–1.0 (Table 3, Fig. 6a) (Turkina, 2005). These compositional characteristics are similar to those of the tonalite–trondhjemite–granodiorite association (TTG), which is widespread in Early Precambrian provinces (Martin, 1994). However, they differ from typical Archean TTG in variably higher concentrations of the most incompatible elements, Rb, Ba, and Th. The rocks of the Uda pluton, mainly quartz diorites and monzodiorites, are in general more melanocratic and display a clear tendency of an increase in K_2O and total alkalis with increasing

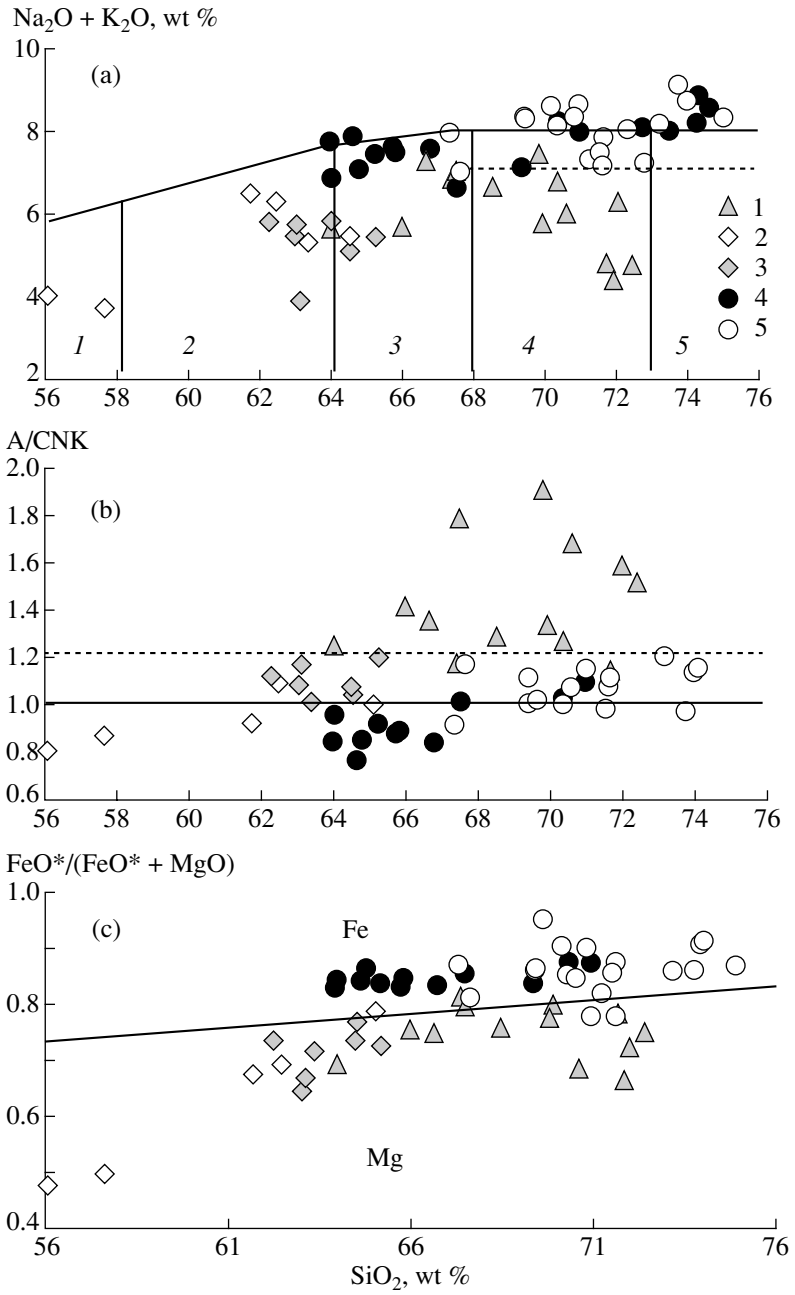

Fig. 4. Diagrams of variations in (a) $Na_2O + K_2O$–SiO_2, (b) A/CNK–SiO_2, and (c) FeO*/(FeO* + MgO)–SiO_2 for the Early Proterozoic granitoids. Granitoids: (*1*) S-type gneissic granites of the border zone of the Tarak massif; (*2*) I-type, Uda massif; (*3*) I-type, Podporog massif; (*4*) A-type, Shumikha massif; and (*5*) A-type, Tarak (central part), Podporog, and Uda massifs. (a) Fields: 1, diorites; 2, quartz diorites; 3, granodiorites and tonalites; 4, granites; and 5, leucogranites. (b) A/CNK = $Al_2O_3/(CaO + Na_2O + K_2O)$, mol % (Clarke, 1981). The solid and dashed lines show the fields of moderately and strongly peraluminous compositions. (c) The boundary between ferroan (Fe) and magnesian (Mg) granitoids is given after Frost et al. (2001a).

SiO_2 content. The increase in K_2O is not accompanied by significant changes in the distribution of REE and high field strength elements, and the dioritoids of the Uda massif are similar to the tonalites of the Podporog pluton in high $(La/Yb)_n$ and Sr/Y values of 11–29 and 15–25, respectively, and a slight negative Eu anomaly, Eu/Eu* = 0.7–1.1 (Table 3, Fig. 6a). The multielement patterns of these granitoids display only negative anomalies in Nb (Ta) and Ti, whereas negative anomalies in Ba, Sr, and P are either lacking or very small (Fig. 7a).

The third group is the most common. It includes the subalkaline granites and leucogranites of the Tarak massif (~1840 Ma), the granitoids of the Shumikha massif, and the subalkaline granites and leucogranites

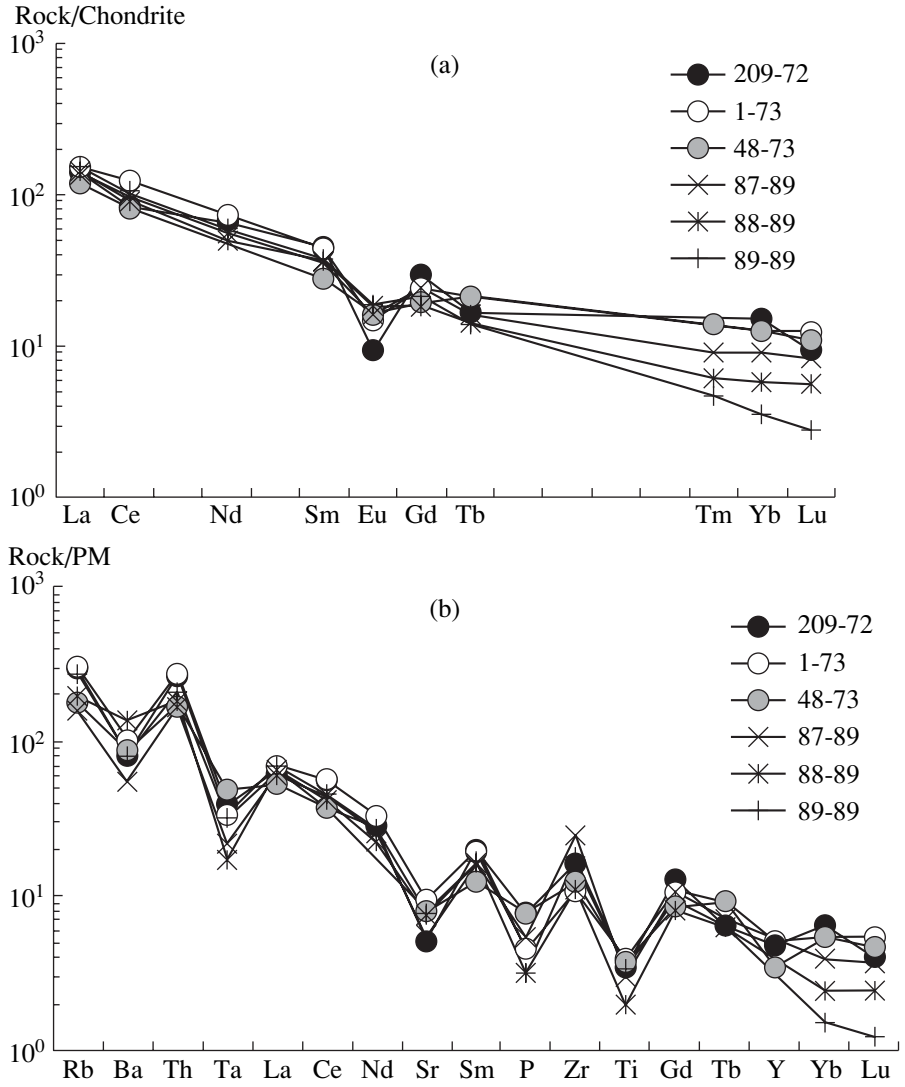

Fig. 5. Distribution of (a) rare earth elements and (b) trace elements in the S-type granites of the Tarak massif (sample numbers correspond to those in Table 3) and the enclosing migmatites (samples 87-89, 88-89, and 89-89). Hereafter, the concentrations are normalized to the chondrite (Boynton, 1984) or primitive mantle (PM) compositions (Sun and McDonough, 1989).

of the Uda massif, which were formed during the post-collisional stage, as well as the intraplate granites and leucogranites of the Podporog intrusion (~1750 Ma). This group is dominated by granites and leucogranites, except for the Shumikha massif, which hosts a wide spectrum of rocks with different SiO_2 contents, from quartz diorite to leucogranite. The granitoids are distinguished by high *f* values (0.75–0.90) (Fig. 4). They belong to the normal or subalkaline series with potassium enrichment over sodium and have metaluminous or slightly peraluminous compositions (Fig. 4). The granitoids of this group show the highest concentrations of REE, Th, and high field strength elements (Zr, Hf, Nb, Ta, and Y) (Tables 3, 4). All these features are characteristic of A-type granites (Whalen et al., 1987; Eby, 1990). The multielement patterns of these granitoids show distinct negative anomalies in Ba, Nb, Sr, P, and Ti (Fig. 7b). The distribution of REE is moderately fractionated with high contents of both light and heavy REE and a pronounced negative Eu anomaly (Eu/Eu* = 0.1–0.4) (Fig. 6b). A weaker negative Eu anomaly is observed in the REE distribution patterns of the Uda granites (Eu/Eu* = 0.5–0.9) (Table 3, Fig. 6b). This group also includes the granitoids of the Barbitai and Girgintuiskii massifs (Tables 1, 4).

Isotopic Systematics of Granitoids

The granitoids show a number of common features in Nd isotopic composition (Table 5). All the igneous rocks have negative ε_{Nd} values, and their model ages are 500–1000 Myr older than the time of rock formation, which suggests that they were derived from sources with a long crustal residence time. A comparison of the

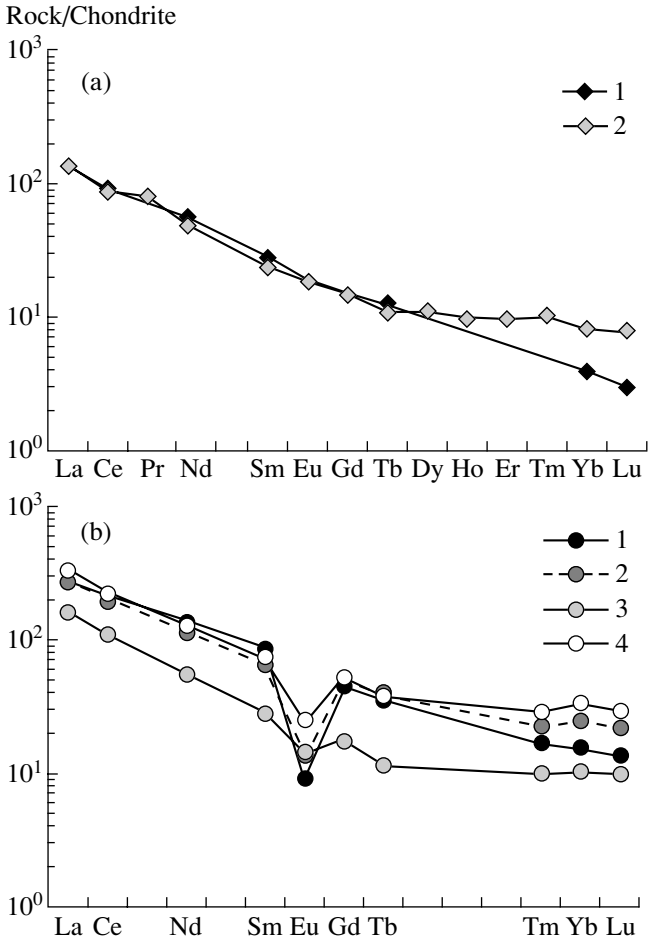

Fig. 6. Distribution of rare earth elements in the granitoids of the (a) I and (b) A types. (a) (1) Podporog and (2) Uda massifs. (b) (1) Tarak, (2) Podporog, (3) Uda, and (4) Shumikha massifs. The diagram shows average compositions for particular massifs.

model ages of the granitoids and the metamorphic country rocks shows that they are similar but not identical. The only exception is the syncollisional garnet-bearing granite of the border zone of the Tarak massif (S-type), whose Nd isotopic characteristics correspond to the country paragneisses and migmatites from the contact zone. In each crustal block, the model ages of I- and A-type granitoids are lower than those of the para- and ortho-gneisses of the enclosing metamorphic complexes; the maximum difference was established between the rocks of the Shumikha massif and the tonalite–trondhjemite gneisses of the Onot block. Correspondingly, the igneous rocks have a more radiogenic Nd isotopic composition (higher ε_{Nd}) than their potential crustal magma sources, the isotopic parameters of which can be estimated from the country rock complexes (Fig. 8). Such relationships suggest a contribution of juvenile mantle material into the magma generating zone, which was dominated by crustal sources.

GENESIS OF GRANITOIDS

Analysis of the Sources and Conditions of Melt Formation

The genesis of various petrological and geochemical types of granitoids is analyzed using the model of melting of metasedimentary (S-type) and metaigneous (I- and A-types) sources (Chappell and White, 1974; Whalen et al., 1987). More comprehensive estimates of the possible compositions of sources can be obtained from the geochemical and isotopic characteristics of the granitoids.

The character of magma-forming material is most obvious for the S-type granites of the border zone of the Tarak pluton, which contain aluminous minerals typical of the country gneisses and migmatites (garnet and cordierite), are similar in multielement patterns to the migmatites, and have Nd isotopic characteristics (ε_{Nd} = –3.1) identical to those of paragneisses and migmatites from the contact zone (ε_{Nd} from –2.8 to –3.1). The observed regular variations in major- and trace-element concentrations with increasing SiO_2 content in the granitoids (depletion in K_2O, Rb, Th, heavy REE, and Y and a decrease in the magnitude of the negative Eu anomaly) are not consistent with the behavior of these components during the differentiation of a single melt, because plagioclase must be the main fractionating phase. The tendency of a decrease in the concentration of K_2O and Rb and in the magnitude of the negative Eu anomaly and an increase in $CaO + Na_2O$ with increasing SiO_2 content can be related to a rise in H_2O activity, which results in the dominant melting of plagioclase and stabilization of micas (Patino Douce and Harris, 1998). The rocks of the Tarak massif are chemically significantly different from the leucocratic melts obtained in experiments on the melting of pelites and aluminous pelites (cordierite–biotite gneisses) with MgO < 2.1 wt % and Fe_2O_3 < 3 wt % (Patino Douce and Johnston, 1991; Koester et al., 2002). In this connection, the high concentrations and variations in the distribution of major (MgO = 1.0–2.8 wt % and Fe_2O_3 = 4–7 wt %) and trace elements (REE, Th, and Zr) in the granitoids can be explained by the variable degree of separation of eutectoid granite melt from the residual minerals, including accessory phases (restite-unmixing model by Chappell et al., 1987). The identity of the residual aluminous phase during metapelite and metagraywacke melting is controlled by pressure with a change from cordierite to garnet at P = 5 kbar (Vielzeuf and Montel, 1994). The coexistence of residual cordierite and garnet in granitoids is possible during melting of cordierite-bearing gneisses, and the experimental data of Koester et al. (2002) constrained the melt generation conditions as P > 5 kbar and T < 850°C. The distribution of Rb, Ba, and Sr in S-type granites provides insight into the role of various phases in melting reactions and the character of the metaterrigenous source of melt, because melting limited by the amounts of biotite and plagioclase produces liquids with high and low

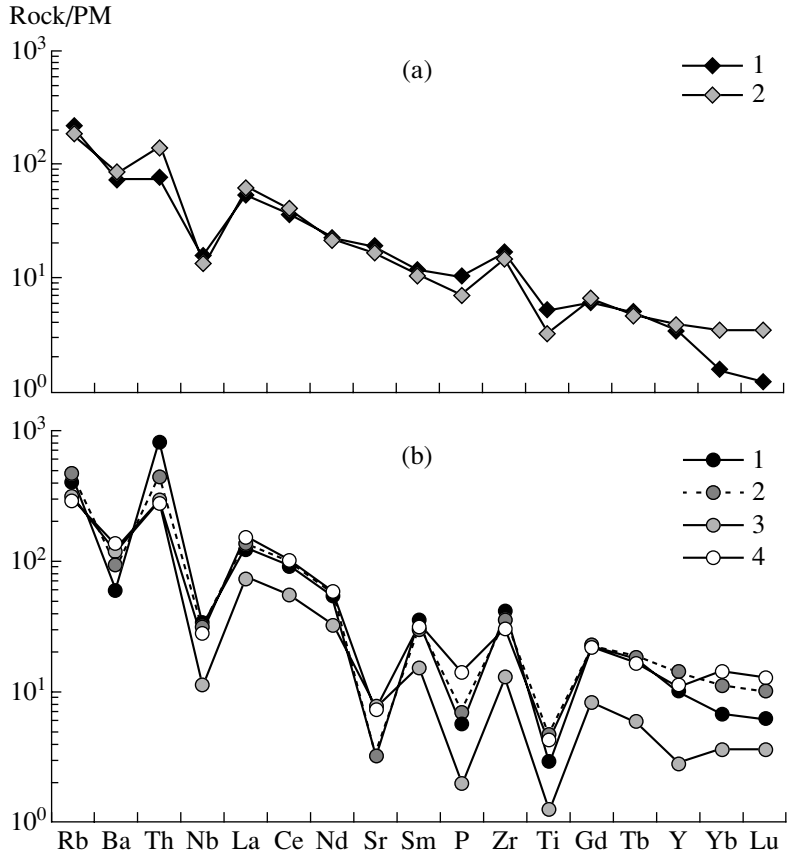

Fig. 7. Trace-element distribution patterns for the granitoids of the (a) I and (b) A types. Symbols are the same as in Fig. 6.

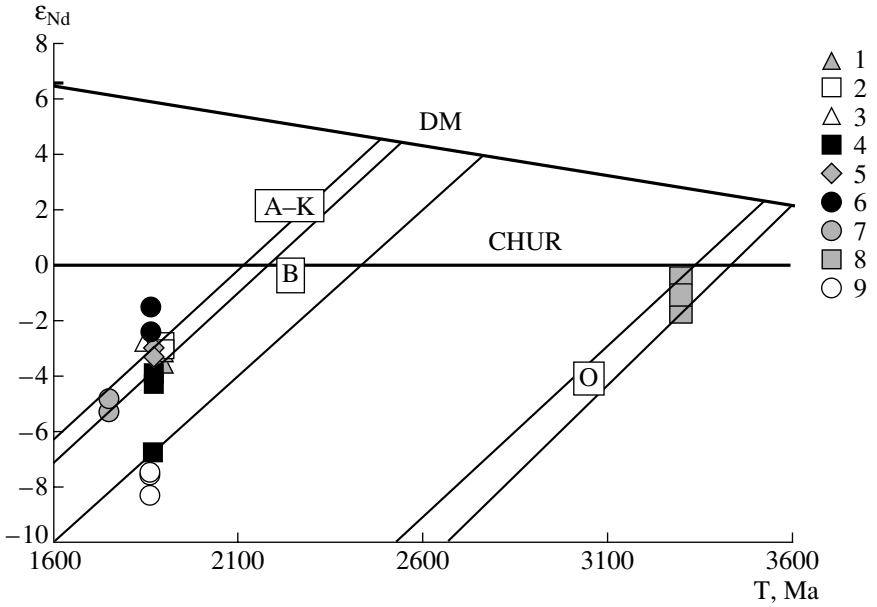

Fig. 8. Diagram of ε_{Nd} versus T for the granitoids and country gneisses. Angara–Kan block (A–K): (1) gneisses, (2) S-type granites and migmatites, (3) A-type granites. Biryusa block (B): (4) gneisses, (5) I-type granites of the Podporog massif, (6) Uda massif, (7) A-type granites of the Podporog massif. Onot block (O): (8) plagiogneisses and (9) Shumikha massif. DM is the depleted mantle, and CHUR is the chondritic uniform reservoir.

Table 5. Isotopic characteristic of Sm and Nd in the Early Proterozoic granitoids and country rocks of the southwestern margin of the Siberian craton

Sample no.	Sm, ppm	Nd, ppm	$^{147}Sm/^{144}Nd$	$^{143}Nd/^{144}Nd$	T, Ma	T(DM), Ma	ε_{Nd}	Rock (massif)
Angara–Kan block								
84-72	6.8	39.0	0.10102	0.511259 ± 10	1840*	2547	–4.3	orthogneiss
101-72	9.36	52.35	0.1080	0.511370 ± 4	1900*	2556	–3.1	paragneiss
89-89	6.27	34.37	0.110290	0.511415 ± 11	1900*	2547	–2.8	migmatite
48-73	5.73	33.15	0.104440	0.511328 ± 12	1900*	2531	–3.1	granite (T) S
1-98	9.26	53.5	0.10456	0.511379 ± 7	1840	2464	–2.8	granite (T) A
Biryusa block								
33-81	5.44	30.13	0.109133	0.511212 ± 13	1870*	2811	–6.8	orthogneiss
38-81	5.87	32.68	0.108626	0.511336 ± 11	1870*	2620	–4.3	orthogneiss
9-00	6.47	31.18	0.105162	0.511311 ± 8	1870*	2572	–3.9	paragneiss
20-00	7.04	40.47	0.10510	0.511355 ± 3	1870	2608	–3.2	tonalite (P) I
21-00	1.77	9.04	0.11827	0.511510 ± 11	1870	2509	–3.1	tonalite (P) I
17-01	4.06	23.41	0.104898	0.511436 ± 18	1860	2392	–1.5	diorite (U) I
33-01	3.76	24.22	0.093839	0.511256 ± 24	1860	2400	–2.4	granite (U) A
17-00	12.52	71.74	0.10548	0.511321 ± 4	1750	2565	–5.3	granite (P) A
14-00	12.0	68.35	0.10621	0.511355 ± 17	1750	2535	–4.8	granite (P) A
Onot block								
63-95	3.08	18.56	0.100214	0.510476 ± 10	1860*	3564	–19.2	plagiogneiss
48-95	1.29	9.97	0.078295	0.509955 ± 15	1860*	3568	–23.9	plagiogneiss
48-03	1.85	10.29	0.108692	0.510695 ± 27	1860*	3537	–17.0	plagiogneiss
173-95	3.19	19.98	0.09643	0.510390 ± 4	1860*	3560	–19.9	plagiogneiss
3-03	16.45	89.92	0.110589	0.511159 ± 19	1860	2927	–7.5	quartz diorite (Sh) A
6-03	15.27	88.65	0.104101	0.511121 ± 24	1860	2807	–8.3	granodiorite (Sh) A
91614[1]	9.25	50.0	0.1119	0.511220 ± 6	1860	2962	–7.5	granite (Sh) A
9060B[1]	18.4	109.8	0.1013	0.511092 ± 4	1860	2959	–7.4	granite (Sh) A

Note: T is the age of granitoids or time (*) accepted for the calculation of ε_{Nd}. Massifs: **T**, Tarak; **P**, Podporog, **U**, Uda; and **Sh**, Shumikha. S, I, and A are petrological and geochemical types of granitoids.
[1] Data of T.V. Donskaya (Institute of the Earth's crust, Siberian Division, Russian Academy of Sciences, Irkutsk).

Rb/Sr and Ba/Sr ratios, respectively (McDermott et al., 1996). The moderate Rb/Sr (0.6–1.8) and Ba/Sr (3.1–5.2) ratios of the granitoids suggest that the melting was controlled by the presence of plagioclase and biotite in the source, which could consist of a mixture of pelitic and graywacke materials. This conclusion is consistent with the existence of corresponding fertile sources in the section of the Angara–Kan block, garnet–biotite and aluminous gneisses, the protoliths of which were pelites and graywackes (Nozhkin and Turkina, 1993).

The I-type granitoids could be derived from crustal metaigneous sources or by the differentiation of more mafic melts; the latter mechanism is more common in subduction settings. According to experimental data, I-type granitic melts can be formed by melting of mafic and intermediate protoliths (Carroll and Wyllie, 1990; Beard and Lofgren, 1991; Rapp and Watson, 1995; Zharikov and Khodarevskaya, 1995; Singh and Johannes, 1996). The variable relative depletion of the rocks of the Podporog and Uda massifs in heavy REE and Y suggests equilibrium of melts with garnet-bearing (tonalites) or garnet-free (dioritoids) residues, which implies melting at pressures higher and lower than 10 kbar, respectively (Beard and Lofgren, 1991; Rapp and Watson, 1995; Singh and Johannes, 1996). In accordance with the experimental data of Beard and Lofgren (1991), the weakly peraluminous character of the tonalites (A/CNK = 1.0–1.2) and the metaluminous character of the dioritoids (0.8–1.1) suggest that the former were derived under higher H_2O activity. The high concentrations of K_2O, Th, and Rb in the rocks compared with average Archean TTG (Martin, 1994) are consistent with a diorite–tonalite rather than mafic source material. The negative ε_{Nd} values in the rocks of this geochemical type also strongly support the contribution from a source with a long crustal residence time.

On the other hand, similar to many I-type granites, the isotope geochemical data provide evidence for the importance of crust–mantle interaction in granite formation. The contributions of recycled (crustal) and juvenile (mantle) materials were estimated on the basis of the binary mixing model. The fraction of the mantle component was calculated by the equation of Jahn et al. (2000)[1]. The procedure of modeling is similar to that used by other authors (e.g., Kerr and Fryer, 1993) and was described in detail by Turkina (2005). It was assumed that the mantle component had ε_{Nd} = +6 and Nd = 10 ppm, corresponding to basalts with weakly fractionated REE distribution patterns derived from a depleted mantle source with an age of 1.87 Ga. The isotopic parameters of the probable crustal sources of silicic melts were estimated from the corresponding characteristics of the Early Precambrian ortho- and para-gneisses of the Biryusa block, which show variable ε_{Nd} values (from –6.8 to –3.9) and an average Nd content of ~30 ppm (Table 5). Depending on the accepted isotopic parameters of the crustal source, the contribution of juvenile basic material to the formation of magmas could be from 25 to 55% for the tonalites of the Podporog massif and 50–70% for the dioritoids of the Uda pluton (Fig. 9). The higher fraction of basic material for the rocks of the Uda massif is consistent with their more melanocratic composition. On the other hand, the dioritoids of the Uda massif and the tonalites of the Podporog massif show similar contents of incompatible elements (Rb, Ba, Sr, Th, and REE). This allows us to suppose that the mantle component contributing to the formation of the rocks of the Uda massif corresponded in composition to basic rocks of the calc-alkaline or subalkaline series enriched in these elements.

The formation of A-type granites is explained by (1) fractionation of alkali basalt melts (Eby, 1990), (2) partial melting of ferrodiorites or basic rocks related to underplating of mantle melts (Frost et al., 2001a, 2001b), and (3) melting of lower crustal tonalite or diorite, which could be affected by previous melting or dehydration episodes (Collins et al., 1982; Creaser et al., 1991; Landenberger and Collins, 1996). Experiments on the dehydration melting of biotite- and amphibole-bearing tonalite gneisses demonstrated that, in principle, melts with major-element compositions corresponding to A-type granites can be derived at P = 6–10 kbar and T = 900–1075°C (Skjerlie and Johnston, 1993). The granitoids studied show high Y/Nb (1.1–3.9) and Yb/Ta (1.3–5.0) ratios, which is characteristic of melts produced from sialic sources (Eby, 1990), whereas the derivatives of basic magmas have low Y/Nb and Yb/Ta (<1.2) ratios approaching those of ocean-island basalts (~0.6). In the Ce/Ta versus Yb/Ta diagram, the compositions of the granitoids tend to plot near the average compositions of the enclosing gneisses of the corresponding crustal block (Fig. 10). The rocks of the Uda and Shumikha massifs form arrays extending toward the average compositions of ocean island basalts (OIB); they can in part reflect a decrease in these ratios during crystal fractionation, but more likely they result from a more significant contribution of mafic material enriched in high-field-strength elements (Ta) into the magma source region. On the other hand, the granitoids of the two massifs show high Ba concentrations, which are up to 1100–1400 ppm in the least evolved varieties and much higher compared with the rocks of the Tarak and Podporog massifs (460–900 ppm). Biotite is the main host of Ba in the residue during melting of a tonalite–gneiss source (Skjerlie and Johnston, 1993). Therefore, the relative enrichment of Ba could be related to the higher temperatures of formation of the granitoids of the Uda and Shumikha massifs, because the stability of residual biotite depends on melting temperature. Another possible reason for the elevated Ba contents in the granitoids is the contribution of a mafic source material corresponding to OIB, which is enriched in Ba (350 ppm Ba according to Sun and McDonough, 1989) compared with basalts from island-arc and spreading environments.

The derivation of melts from ancient crustal sources is also supported by the low negative ε_{Nd} values of the granitoids. The isotope geochemical parameters of possible crustal sources of the silicic melts were estimated from the corresponding characteristics of the enclosing Early Precambrian gneiss complexes (Table 5). These rocks are represented by orthogneisses of andesite compositions, paragneisses, and migmatites (ε_{Nd} from –3.5 to –4.3 and 35 ppm Nd) in the Angara–Kan block; para- and orthogneisses (metadacites) (ε_{Nd} from –6.8 to –3.9 and 30–50 ppm Nd) in the Biryusa block; and plagiogneisses of tonalite–trondhjemite compositions (ε_{Nd} from –17 to –20 and 15–19 ppm Nd) in the Onot block. As was mentioned above, the granitoids of all the massifs show higher ε_{Nd} values (–2.8 in the Tarak massif, from –4.8 to –5.3 in the Podporog massif, –2.4 in the Uda massif, and from –7.4 to –8.3 in the Shumikha massif) than their possible crustal sources, which suggests a contribution of juvenile mantle material to the formation of granites. The relative amount of the juvenile material was estimated assuming Nd = 15 ppm and ε_{Nd} = +6 for the mantle component corresponding to basalts with weakly fractionated REE distribution patterns derived from a depleted mantle reservoir with an age of 1.87 Ga. The results of these calculations are shown in Fig. 9. Given these parameters, the fraction of the juvenile basic component in the source region ranges from the minimum values of 0–35% for the granites of the Podporog and Tarak massifs to 40–50% for the rocks of the Uda and Shumikha massifs. In addition to isotopic data, the higher fraction of basic mate-

[1] $X_m = [(\varepsilon_c - \varepsilon_{mx})Nd_c]/[\varepsilon_{mx}(Nd_m - Nd_c) - (\varepsilon_m Nd_m - \varepsilon_c Nd_c)]$, where ε_{mx}, ε_c, and ε_m are the ε_{Nd} values for the resulting mixture (granitoid, crustal component, and mantle component, respectively); Nd_c and Nd_m are the concentrations of Nd in the crustal and mantle components, respectively; and X_m is the fraction of the mantle component.

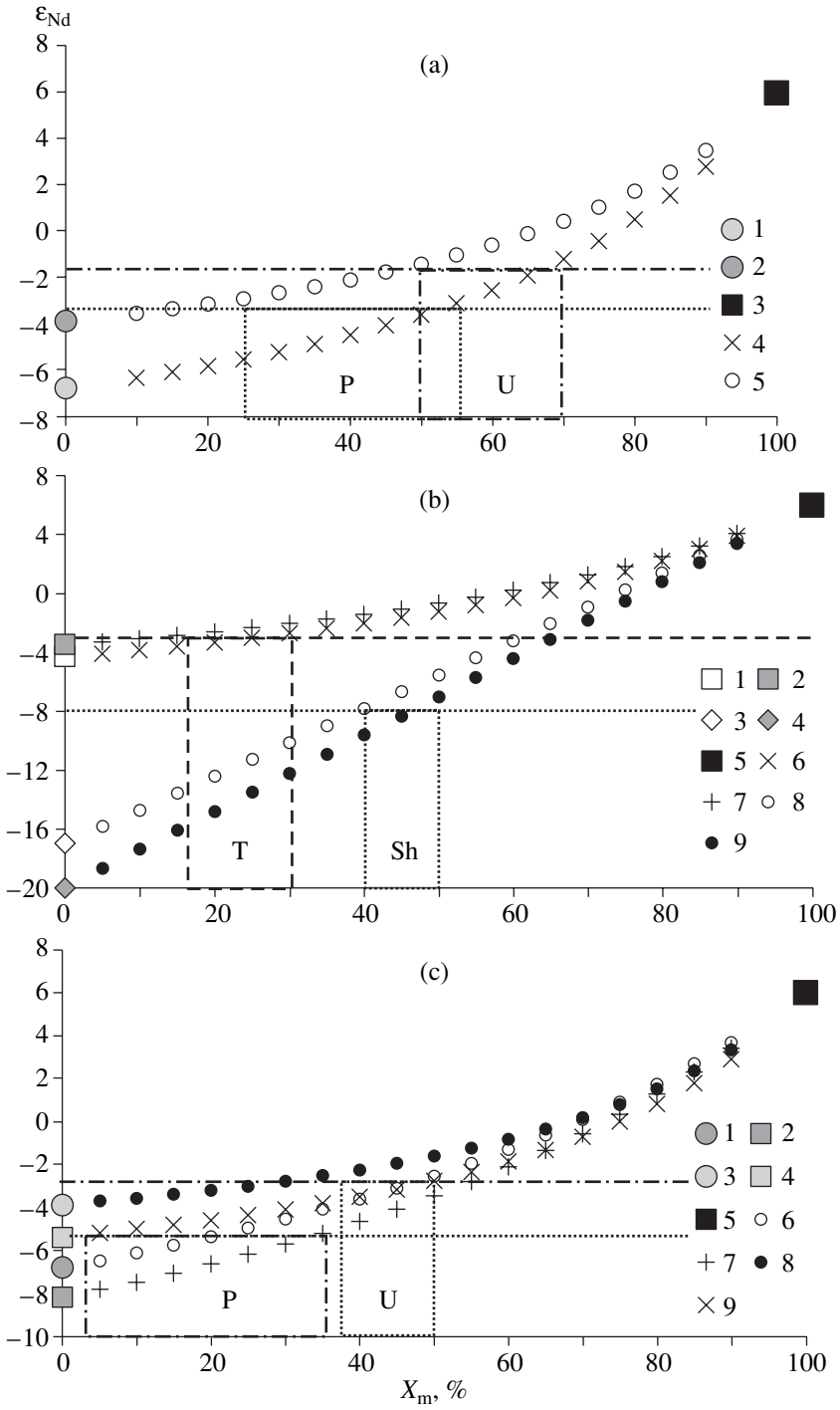

Fig. 9. Diagram of ε_{Nd} versus the fraction of mantle component (X_m, %). Curves show variations in the Nd isotopic composition during the formation of granitoids by mixing of crustal and juvenile basic components. Horizontal lines correspond to the average Nd isotopic compositions of granitoids from particular massifs. (a) I-type granites of the Biryusa block. (1) and (2) isotopic compositions of the crust of the Biryusa block, (3) mantle component, (4) and (5) mixing lines for a Nd content of 30 ppm and ε_{Nd} values of –6.8 and –3.9 in the crustal component. Fields show the contributions of the mantle component to the formation of the tonalites of the Podporog massif (P) and the dioritoids of the Uda massif (U). Hereafter, see text for further explanation. (b) A-type granites of the Angara–Kan and Onot blocks. The isotopic compositions of crustal components: (1) and (2) Angara–Kan block; (3) and (4) Onot block; (5) mantle component; (6)–(9) mixing lines for various contents of Nd and ε_{Nd} values in crustal components. Fields correspond to the contribution of the mantle component into the formation of the granitoids of the Tarak (T) and Shumikha (Sh) massifs. (c) A-type granites of the Biryusa block. The isotopic compositions of crustal components for ages of (1) and (2) 1.75 Ga; (3) and (4) 1.87 Ga; (5) mantle component; (6)–(9) mixing lines for various Nd contents and ε_{Nd} values in crustal components. Fields show the contributions of the mantle component into the formation of the granitoids of the Podporog (P) and Uda (U) massifs.

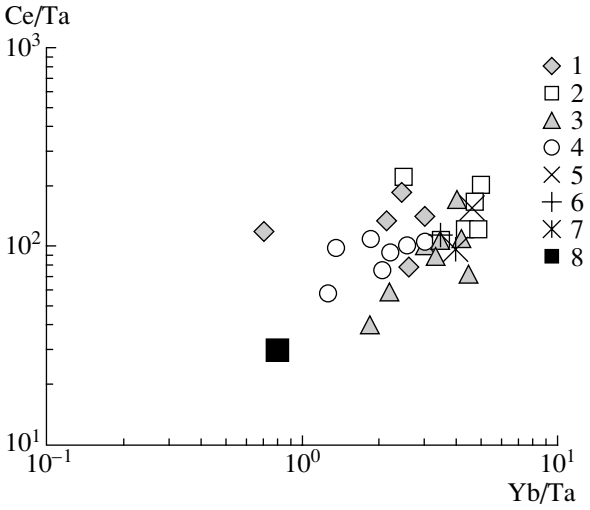

Fig. 10. Diagram of Ce/Ta versus Yb/Ta for the Early Proterozoic A-type granitoids. Massifs: (1) Tarak, (2) Podporog, (3) Shumikha, and (4) Uda. Also shown are the average compositions of the country gneisses of the (5) Angara–Kan, (6) Biryusa, and (7) Onot blocks and (8) the average composition of ocean island basalts (Sun and McDonough, 1989).

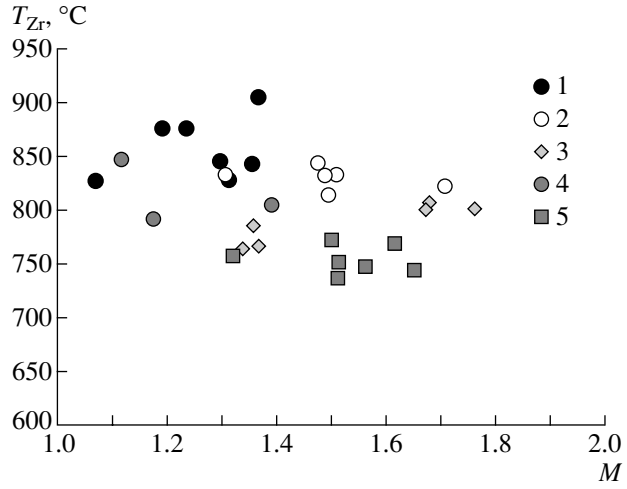

Fig. 11. Calculated temperatures of zircon crystallization for the Early Proterozoic granitoids. A-type granites of (1) Tarak, (2) Podporog, (3) Shumikha, and (4) Uda massifs; and (5) I-type granites of the Podporog and Uda massifs. M = (Na + K + 2Ca)/(Al × Si) (cation ratio) (Watson and Harrison, 1983).

rial for the formation of granitoids from the Uda and Shumikha plutons is supported by elevated Ba concentrations in these rocks suggesting a possible contribution from an OIB-type mantle source. In addition, the rocks of the Shumikha pluton have the most melanocratic compositions.

Temperatures of Granitoid Formation

The temperature conditions of granitoid formation were estimated by the calculation of zircon saturation temperatures for melt crystallization (Watson and Harrison, 1983), which reflect to a first approximation the possible conditions of melt generation. The absence of monazite in the majority of granitoids hampers the estimation of temperature from the saturation in lanthanide phases (Montel, 1993), and, consequently, the convergence of the obtained values cannot be checked. Exceptions are the monazite-bearing granites of the Tarak massif, which yielded similar temperature ranges (T_{Zr} = 830–910°C and T_{REE} = 870–950°C) at an H_2O content of 4 wt %. The calculated temperatures are shown in Fig. 11. The iron-poor magnetite-bearing tonalites and diorites of the Podporog and Uda massifs (I type), which probably crystallized from a water richer melt at high O_2 activity, show lower temperatures (670–770°C) compared with the iron-rich and more reduced A-type granites from all the massifs (800–920°C). The temperature values obtained for the A-type granites approach the conditions of formation of such magmas inferred from experimental data (>950°C at P = 10 kbar) (Skjerlie and Johnston, 1993). Lower crystallization temperatures of 750–770°C were obtained for the amphibole–plagioclase assemblage (Holland and Blundy, 1994) from the A-type granites of the Shumikha massif at P = 4 kbar, which indicates later crystallization of these minerals compared with zircon.

Factors Controlling the Diversity and Specific Features of the Compositions of Granitoids in Collisional Settings

It is well known (e.g., Förster et al., 1997) that the composition and isotope geochemical characteristics of granitoids reflect primarily the corresponding parameters of their sources rather than the geodynamic setting of their formation. In our case this is supported by the negligible differences between the A-type granites of postcollisional and intraplate settings. Accordingly, the diversity of petrological and geochemical types of felsic igneous rocks in collisional orogens can be primarily attributed to the presence in the thickened crustal sections of these structures of tectonically juxtaposed rock complexes varying in composition and origin and serving as fertile sources for the generation of silicic melts. When sedimentary and igneous complexes are buried to depths sufficient for melting (middle and lower crust), S-, I- and A-type granites can be formed nearly synchronously by melting of the crustal section at various levels. What is the role of the melt source? Which chemical criteria can be used for the identification of magma-forming materials for various types of granitoids? In our case, an obvious criterion for S-type granites is the presence of aluminous mineral phases, garnet and cordierite, and the possibility of direct derivation of these rocks from the material of the host paragneiss complex is demonstrated by their identical Nd isotopic characteristics. The tonalites and dioritoids

of the Podporog and Uda massifs (I-type granites) have low concentrations of incompatible elements, high CaO and Sr contents, and negative ε_{Nd} values, which suggest that they were derived mainly from a low-potassium but not metabasic source. This source could be composed of diorite–tonalite or plagiogneiss material, which is in agreement with the experimental data of Singh and Johannes (1996). The nature of crustal sources for A-type granites is more difficult to constrain, at least for the plutons of the Angara–Kan and Biryusa blocks, whose sections include strongly metamorphosed para- and orthogneisses showing similar levels of incompatible trace element contents and negligible differences in Nd isotopic composition (Table 5). Most likely, the trace element composition of A-type granites depends on the composition of the crust on the whole. The highest concentrations of Th (40–60 ppm), Zr, and light REE in the A-type granites of the Angara–Kan and Biryusa blocks correlate with the enrichment of these elements in the country granulite gneisses (17.6 and 15.6 ppm Th, respectively) (Nozhkin and Turkina, 1993). Much lower Th concentrations were detected in the rocks of the Shumikha massif and the tonalite–trondhjemite gneisses of the Onot block, 24.2 and 3.6 ppm, respectively (Nozhkin et al., 2001). Of course, the contribution of the juvenile mantle component into granite formation is not accounted for in this correlation.

According to experimental data, I- and A-type granites can be derived by melting of chemically almost identical diorite–tonalite and plagiogneiss materials. An important factor controlling the formation of these two types of melt is water activity, which is related to redox conditions controlling the FeO*/(FeO* + MgO) ratio of the melt. In this aspect, the distinguishing of two granitoid series is of fundamental importance (Frost et al., 2001a): the magnesian series is related to water richer environments and calc-alkaline sources, and the ferroan series is correlated with dry conditions and tholeiitic magmas. This allows a reliable discrimination of A- and I-type granites (Fig. 4). In addition, the I- and A-type granites studied are distinctly different in crystallization temperature, which is certainly correlated with melt generation temperature. As to the pressure of melt generation, the depletion of heavy REE and Y in the tonalites and diorites suggests the presence of garnet and amphibole in the residue and, consequently, deep lower crustal melting conditions (Turkina, 2005). Pressure cannot be constrained for the A-type granites because of the absence of pressure indicator phases in the residues. Garnet appears during the incongruent melting of biotite (P = 10 kbar), but it is rapidly consumed in subsequent melting reactions at T ~ 950°C, and orthopyroxene is the only femic mineral within the reasonable P–T range (Skjerlie and Johnston, 1993).

The coexistence of different granitoid types forming under contrasting T–α_{H_2O} conditions in the same massifs is probably not accidental and provides some constraints on the processes of their formation. In two cases (Tarak and Podporog massifs), isotopic data suggested the later generation of A-type granites. They were probably derived at a crustal level not yet depleted by the generation of earlier granitoid magmas, i.e., the source material was fertile but experienced dehydration, which provided low water activity and high temperature of melt formation during late stages of granite formation. A similar scenario was proposed for the sequential generation of I- and A-type granites in the Chaelundi complex, Eastern Australia (Landenberger and Collins, 1996): the formation of I-type granites caused dehydration of the lower crust, from which A-type granites were subsequently derived.

Role of Crust–Mantle Interaction in Granite Formation

Experimental data and the obtained estimates of crystallization temperature show that the silicic melts parental for the I- and A-type granitoids were formed at temperatures significantly above the eutectic. This evidently requires an external heat source for the initiation of melting. In addition to radiogenic heating, underplating of basic melts at the base of the crust is a potential heat source under extensional conditions developing during the late stage of the evolution of a collisional orogen (Sylvester, 1998; Huppert and Sparks, 1988). If there is no data on the occurrence of mafic magmatism coeval with granite formation, evidence for underplating can be obtained from isotope geochemistry indicating a contribution from juvenile mantle material into the formation of granitoids. As was shown above, the contribution of basic material into the formation of the granitoids was estimated from 0 to 70%. Variations in the fraction of mafic material in granite source regions are strongly correlated with the concentrations of major and trace elements in granitoids: the maximum fraction of mantle material was obtained for the most mafic varieties of the Uda and Shumikha massifs. The model of binary mixing rather than assimilation and fractional crystallization of a mafic melt is evidently a plausible approximation, which is suggested by the isotopic systematics of Shumikha rocks showing the widest compositional range (diorites, granodiorites, and granites). The ε_{Nd} values of four samples with different SiO_2 contents vary within a narrow range of 1 and exhibit no correlation with SiO_2 or other petrochemical parameters, which suggests that the mixing occurred at the level of melt generation.

Thus, the evolution of the collisional orogen involved recycling of the ancient continental crust and input of juvenile material under extensional conditions caused by the instability of the thickened crust and thinning of the lithosphere owing to delamination, which initiated underplating of basic melts at the base of the crust. The thermal influence of mantle melts was probably the main factor responsible for the large-scale granite formation under collisional conditions.

CONCLUSIONS

(1) The formation of Early Proterozoic granitoids in the southwestern margin of the Siberian craton was related to collisional events. Three stages of granite formation were distinguished: (1) syncollisional stage, involving the formation of granitoids in the border and contact zones of the Tarak massif; (2) postorogenic or postcollisional stage, producing numerous granitoid plutons of diverse composition; and (3) intraplate stage, including the formation of the potassic granites of the Podporog massif. In terms of mineral and chemical compositions, the granitoid massifs are made up of three petrological and geochemical rock types: S, I, and A.

(2) The S-type granites have peraluminous compositions and bear aluminous mineral phases (garnet and cordierite); their trace element distribution patterns are similar to those of the country paragneisses and migmatites, and the Nd isotopic compositions are identical to those of the latter. The S-type granitoids were derived by melting under variable H_2O activity of aluminous and garnet–biotite gneisses at $P \geq 5$ kbar and $T < 850$°C with a varying degree of melt separation from the residual phases.

(3) The I-type tonalites and dioritoids show low FeO*/(FeO* + MgO) ratios, high concentrations of CaO and Sr, fractionated REE distribution patterns, $(La/Yb)_n = 11–42$, and variable degree of heavy REE depletion, which increases toward tonalites. Their parental melts were formed at $T \geq 850$°C and $P >$ 10 kbar (tonalites) or $P < 10$ kbar (dioritoids). Isotopic data suggest that their formation was related to the melting of a Late Archean crustal (tonalite–diorite–gneiss) source with the contribution of juvenile material ranging from 25–55 (tonalites of the Podporog massif) to 50–70% (dioritoids of the Uda pluton).

(4) The predominant A-type granitoids show the highest FeO*/(FeO* + MgO) ratios; high concentrations of high-field-strength elements, Th, light REE, and heavy REE; and a distinct negative Eu anomaly. Their primary melts were formed under low H_2O activity and $T \geq 950$°C. The Nd isotopic compositions of the granitoids suggest a role for ancient (Early and Late Archean) crustal (tonalite–diorite–gneiss) sources and juvenile mantle material in magma formation. The contribution of the juvenile material ranges from 0–35% for the granites of the Podporog and Tarak massifs to 40–50% for the rocks of the Uda and Shumikha plutons.

(5) The main factors responsible for the diversity of petrological and geochemical types of granitoids in collisional environments are the existence of various fertile sources in the section of the thickened crust of the collisional orogen, variations in magma generation conditions (α_{H_2O}, T, and P) during sequential stages of granite formation, and variations in the fraction of juvenile mantle material in the source region of granitoid melts.

ACKNOWLEDGMENTS

The authors are grateful to A.A. Delenitsin (Geological Institute, Kola Research Center, Russian Academy of Sciences, Apatity) and I.V. Nikolaeva (Joint Institute of Geology, Geophysics, and Mineralogy, Siberian Division, Russian Academy of Sciences, Novosibirsk), who carried out the trace-element and isotopic analysis of our rock samples. This study was financially supported by the Russian Foundation for Basic Research (project nos. 03-05-64936, 04-05-64301, and 04-05-64179) and Program for Support of Leading Scientific Schools (grant nos. NSh-1573.2003.5 and NSh-2305.2003.5).

REFERENCES

1. Z. M. Anisimova, A. A. Podvezko, and S. V. Cheremisin, *Geological Map of Irkutsk Oblast and Adjacent Territories. Scale 1:500000*, Ed. by V. G. Kuznetsov and P. M. Khrenov (Min. Geol. SSSR, VSEGEI, Leningrad, 1982) [in Russian].
2. S. I. Arbuzov and S. V. Novoselov, "Native Iron in Granites of the Tarak Complex, Southern Yenisei Range," Zap. Vseross. Mineral. O–va **124** (1), 75–78 (1995).
3. T. B. Bayanova, *Age of the Key Geologic Complexes of the Kola Region and Duration of the Magmatic Processes* (Nauka, St. Petersburg, 2004) [in Russian].
4. J. S. Beard and G. E. Lofgren, "Dehydration Melting and Water-Saturated Melting of Basaltic and Andesitic Greenstones and Amphibolites at 1, 3 and 6.9 kbar," J. Petrol. **32**, 365–401 (1991).
5. E. V. Bibikova, T. V. Gracheva, V. A. Makarov, and A. D. Nozhkin, "Age Boundaries in the Early Precambrian Geologic Evolution of the Yenisei Range," Stratigr. Geol. Korrelyatsiya **1** (1), 35–40 (1993).
6. E. V. Bibikova, T. V. Gracheva, I. K. Kozakov, et al., "U–Pb Age of the Hypersthene Granites (Kuzeevites), Angara–Kan Inlier (Yenisei Range)," Geol. Geofiz. **42**, 864–867 (2001a).
7. E. V. Bibikova, V. I. Levitskii, L. Z. Reznitskii, et al., "Archean Tonalite–Trondhjemite Association of the Sayan Region Basement Inlier of the Siberian Platform: U–Pb, Sm–Nd and Sr Isotopic Data," in *Geology, Geochemistry, and Geophysics at the Boundary of the 20th and 21th Centuries* (Inst. Zemn. Kory Sib. Otd. Ross. Akad. Nauk, Irkutsk, 2001b) [in Russian].
8. W. V. Boynton, "Cosmochemistry of the Rare Earth Elements: Meteorite Studies," in *Rare Earth Element Geochemistry*, Ed. by P. Henderson (Elsevier, Amsterdam, 1984), pp. 63–114.
9. V. V. Bryntsev, *Precambrian Granitoids of the Northwestern Sayan Region* (Nauka, Novosibirsk, 1994) [in Russian].
10. M. R. Carroll and P. J. Wyllie, "The System Tonalite–H_2O at 15 kbar and the Genesis of Calc-Alkaline Magmas," Am. Mineral. **75**, 345–357 (1990).
11. B. W. Chappell and A. J. White, "Two Contrasting Granite Types," Pacific Geol. **8**, 173–174 (1974).
12. B. W. Chappell, A. J. White, and D. Wyborn, "The Importance of Residual Source Material (Restite) in Granite Petrogenesis," J. Petrol. **28**, 1111–1138 (1987).

13. D. B. Clarke, "Peraluminous Granites," Can. Mineral. **19**, 1–2 (1981).
14. W. J. Collins, S. D. Beams, A. J. R. White, and B. W. Chappell, "Nature and Origin of A-Type Granites with Particular Reference to Southeastern Australia," Contrib. Mineral. Petrol. **80**, 189–200 (1982).
15. R. A. Creaser, R. C. Price, and R. J. Wormald, "A-Type Granites Revisited: Assessment of the Residual–Source Model," Geology **19**, 163–166 (1991).
16. V. M. Datsenko, *Granitoid Magmatism of the Southwestern Framing of the Siberian Craton* (Nauka, Novosibirsk, 1984) [in Russian].
17. T. V. Donskaya, E. B. Sal'nikova, E. V. Sklyarov, et al., "Early Proterozoic Postcollision Magmatism at the Southern Flank of the Siberian Craton: New Geochronological Data and Geodynamic Implications," Dokl. Akad. Nauk **382**, 663–667 (2002) [Dokl. Earth Sci. **383**, 125–129 (2002)].
18. G. N. Eby, "The A-Type Granitoids: A Review of Their Occurrence and Chemical Characteristics and Speculations on Their Petrogenesis," Lithos **26**, 115–134 (1990).
19. H.-J. Förster, G. Tischendorf, and R. B. Trumbull, "An Evaluation of the Rb vs. (Y + Nb) Discrimination Diagram to Infer Tectonic Setting of Silicic Igneous Rocks," Lithos **40**, 261–293 (1997).
20. B. R. Frost, C. G. Barnes, W. J. Collins, et al., "A Geochemical Classification for Granitic Rocks," J. Petrol. **42**, 2033–2048 (2001a).
21. C. D. Frost, J. M. Bell, B. R. Frost, and K. R. Chamberlain, "Crustal Growth by Magmatic Underplating: Isotopic Evidence from the Northern Sherman Batholith," Geology **29**, 515–518 (2001b).
22. T. Holland and J. Blundy, "Non-Ideal Interactions in Calcic Amphiboles and Their Bearing on Amphibole–Plagioclase Thermometry," Contrib. Mineral. Petrol. **116**, 433–447 (1994).
23. H. Huppert and R. S. J. Sparks, "The Generation of Granitic Magmas by Intrusion of Basalt into Continental Crust," J. Petrol. **29**, 599–624 (1988).
24. B. M. Jahn, F. Wu, and B. Chen, "Massive Granitoid Generation in Central Asia: Nd Isotope Evidence and Implication for Continental Growth in the Phanerozoic," Episodes **23**, 82–92 (2000).
25. A. Kerr and B. J. Fryer, "Nd Isotope Evidence for Crust–Mantle Interaction in the Generation of A-Type Granitoid Suites in Labrador, Canada," Chem. Geol. **104**, 39–60 (1993).
26. T. I. Kirnozova, E. V. Bibikova, I. K. Kozakov, et al., "Early Proterozoic Postcollisional Granitoids in Basement Inlier of the Sayan Region of the Siberian Craton: U–Pb Geochronological and Sm–Nd Isotope Data," in *Proceedings of 2nd Conference on Isotope Geochronology: Isotope Geochronology in the Solution of Problems of Geodynamics and Ore Genesis, St. Petersburg, Russia, 2003* (TsIK, St. Petersburg, 2003), pp. 193–195 [in Russian].
27. E. Koester, A. R. Pawley, A. D. Fernandes, C. C. Porcher, et al., "Experimental Melting of Cordierite Gneiss and the Petrogenesis of Syntranscurrent Peraluminous Granites in Southern Brazil," J. Petrol. **43**, 1595–1616 (2002).
28. T. E. Krogh, "A Low-Contamination Method for Hydrothermal Dissolution of Zircon and Extraction of U and Pb for Isotopic Age Determinations," Geochim. Cosmochim. Acta **73**, 485–494 (1973).
29. B. Landenberger and W. J. Collins, "Derivation of A-Type Granites from a Dehydrated Charnockitic Lower Crust: Evidence from the Chaelundi Complex, Eastern Australia," J. Petrol. **37**, 145–170 (1996).
30. V. I. Levitskii, A. I. Mel'nikov, L. Z. Reznitskii, et al., "Postkinematic Early Proterozoic Granitoids of the Southwestern Siberian Craton," Geol. Geofiz. **43**, 717–731 (2002).
31. K. R. Ludwig, "PbDat for MS-DOS, Version 1.21," U.S. Geol. Surv. Open-File Rept. 88-542, 35 (1991).
32. K. R. Ludwig, "ISOPLOT/Ex—A Geochronological Toolkit for Microsoft Excel. Version 2.05," Berkeley Geochronology Center, Spec. Publ. **1**, 1999.
33. H. Martin, "The Archean Grey Gneisses and the Genesis of Continental Crust," in *Archean Crustal Evolution*, Ed. by K. Condie (Elsevier, Amsterdam, 1994).
34. F. McDermott, N. B. W. Harris, and C. J. Hawkesworth, "Geochemical Constraints on Crustal Anatexis: A Case Study from the Pan-African Damara Granitoids of Namibia," Contib. Mineral. Petrol. **123**, 406–423 (1996).
35. J.-M. Montel, "A Model for Monazite/Melt Equilibrium and Application to the Generation of Granitic Magmas," Chem. Geol. **110**, 127–146 (1993).
36. A. D. Nozhkin and O. M. Turkina, *Geochemistry of Granulites* (Ob'ed. Inst. Geol. Geofiz. Mineral. Sib Otd. Ross. Akad. Nauk, Novosibirsk, 1993) [in Russian].
37. A. D. Nozhkin, E. V. Bibikova, O. M. Turkina, and V. A. Ponomarchuk, "Isotope Geochronological Investigations (U–Pb, Ar–Ar, and Sm–Nd) of Subalkaline Porphyritic Granites of the Tarak Massif of the Yenisei Range," Geol. Geofiz. **44**, 879–889 (2003).
38. A. D. Nozhkin, O. M. Turkina, and M. S. Mel'gunov, "Geochemistry of the Metavolcanosedimentary and Granitoid Rocks of the Onot Greenstone Belt," Geokhimiya, No. 1, 31–50 (2001) [Geochem. Int. **39**, 27–56 (2001)].
39. P. A. Nurmi and I. Haapala, "The Proterozoic Granitoids of Finland: Granite Types, Metallogeny and Relation to Crustal Evolution," Bull. Geol. Surv. Finl. **58**, 203–233 (1986).
40. P. J. Patchett and N. T. Arndt, "Nd Isotopes and Tectonics of 1.9–1.7 Crustal Genesis," Earth Planet. Sci. Lett. **78**, 329–338 (1986).
41. A. E. Patino Douce and N. Harris, "Experimental Constraints on Himalayan Anatexis," J. Petrol. **39**, 689–710 (1998).
42. A. E. Patino Douce and A. D. Johnston, "Phase Equilibria and Melt Productivity in the Pelite System: Implication for the Origin of Peraluminous Granitoids and Aluminous Granulites," Contrib. Mineral. Petrol. **107**, 202–218 (1991).
43. R. P. Rapp and E. B. Watson, "Dehydration Melting of Metabasalt at 8–32 kbar: Implications for Continental Growth and Crust–Mantle Recycling," J. Petrol. **36**, 891–931 (1995).
44. O. M. Rozen and V. S. Fedorovskii, *Collisional Granitoids and Layering in the Earth's Crust* (Nauchnyi Mir, Moscow, 2001) [in Russian].

45. J. Singh and W. Johannes, "Dehydration Melting of Tonalites. Part II. Composition of Melts and Solids," Contrib. Mineral. Petrol. **125**, 26–44 (1996).
46. K. P. Skjerlie and A. D. Johnston, "Fluid-Absent Melting Behavior of an F-Rich Tonalitic Gneiss at Mid-Crustal Pressures: Implications for the Generation of Anorogenic Granites," J. Petrol. **34**, 785–815 (1993).
47. J. S. Stacey and J. D. Kramers, "Approximation of Terrestrial Lead Isotope Evolution by a Two-Stage Model," Earth Planet. Sci. Lett. **26**, 207–221 (1975).
48. S. S. Sun and W. F. McDonough, "Chemical and Isotopic Systematics of Oceanic Basalts: Implications for Mantle Composition and Processes," in *Magmatism in the Oceanic Basins*, Eds. by A. D. Saunders and M. J. Norry., Geol. Soc. Spec. Publ., No 42, 313–345 (1989).
49. P. J. Sylvester, "Post-Collisional Strongly Peraluminous Granites," Lithos **45**, 29–44 (1998).
50. O. M. Turkina, "Proterozoic Tonalites and Trondhjemites of the Southwestern Margin of the Siberian Craton: Isotope Geochemical Evidence for the Lower Crustal Sources and Conditions of Melt Formation in Collisional Settings," Petrologiya **13**, 41–55 (2005) [Petrology **13**, 35–49 (2005)].
51. O. M. Turkina, E. V. Bibikova, and A. D. Nozhkin, "Stages and Geodynamic Settings of Early Proterozoic Granite Formation on the Southwestern Margin of the Siberian Craton," Dokl. Akad. Nauk **388**, 779–783 (2003) [Dokl. Earth Sci. **389**, 159–165 (2003)].
52. D. Vielzeuf and J. M. Montel, "Partial Melting of Metagreywackes. Part I. Fluid-Absent Experiments and Phase Relationships," Contrib. Mineral. Petrol. **117**, 375–393 (1994).
53. E. B. Watson and T. M. Harrison, "Zircon Saturation Revisited: Temperature and Composition Effects in a Variety of Crustal Magma Types," Earth Planet. Sci. Lett. **64**, 295–304 (1983).
54. J. B. Whalen, K. L. Currie, and B. W. Chappell, "A-Type Granites: Geochemical Characteristics, Discrimination and Petrogenesis," Contrib. Mineral. Petrol. **95**, 407–419 (1987).
55. J. B. Whalen, E. C. Symes, and R. A. Stern, "Geochemical and Nd Isotopic Evolution of Paleoproterozoic Arc-Type Granitoid Magmatism in the Flin Flon Belt, Trans-Hudson Orogen, Canada," Can. J. Earth Sci. **36**, 227–250 (1998).
56. V. A. Zharikov and L. I. Khodarevskaya, "Melting of Amphibolites: Compositions of Partial Melts at Pressures of 5–25 kbar," Dokl. Akad. Nauk **341** (6), 799–803 (1995).